
# B0 accelerometers Groningen

## Damping effects by buildings of the B0 accelerometers

State supervision of de Mines (SodM)

9 July 2019

| | |
|---|---|
| **Project** | B0 accelerometers Groningen |
| **Client** | State supervision of de Mines (SodM) |

| | |
|---|---|
| **Document** | Damping effects by buildings of the B0 accelerometers |
| **Status** | Final version |
| **Date** | 9 July 2019 |
| **Reference** | 113982/19-011.388 |

| | |
|---|---|
| **Project code** | 113982 |
| **Project Leader** | |
| **Project Director** | |

| | |
|---|---|
| **Author(s)** | |
| **Checked by** | |
| **Approved by** | |

**Initials**

**Address**

Witteveen+Bos Raadgevende ingenieurs B.V.
Leeuwenbrug 8
P.O. Box 233
7400 AE Deventer
The Netherlands

## TABLE OF CONTENTS

## APPENDICES

# 1

## INTRODUCTION

### 1.1 Background

The Groningen ground motion recording system comprises B-stations which are positioned in buildings and G-stations, which are arrays of accelerometers and geophones positioned in the free field. Recently it has been concluded that B-stations compared to G-stations show a trend of reduced frequency content in the higher frequency range (Seister, 2019). It is concluded that these reductions are only observed for the horizontal ground motion component, represented by means of the geomean horizontal acceleration.

The total dataset of B-station and G-station recordings of Groningen field induced earthquakes forms the basis for development of Ground Motion Models (GMM) that are part of the Groningen Hazard and Risk program. Since the B-stations are the longest operational stations the records from these stations are highly valuable for any Groningen GMM to be developed. For this reason, State supervisor of the Mines (SodM) needs to understand if and how B-stations recordings can be used for GMM-development. The present study is part of this SodM-campaign.

### 1.2 Scope and objectives

The present study addresses possible corrections required to capture so called 'kinematic' effects. Kinematic effects is the term often used in international codes and literature to refer to deviations between free field ground response and foundation input motion response that result from non-synchronous base excitation caused by different arrival times of the waves at different locations of a building foundation. Obviously, these effects are more pronounced for foundations with large dimensions (plan and embedment depth) and massive or rigid foundations.

SodM has requested Witteveen+Bos to conduct a study that has to conclude if the observed deviations for B-stations can be reproduced by means of simplified code-based correction models (NIST (NEHRP Consultants Joint Venture, 2012) and FEMA 440 (NEHRP, 2005)). The aim of this is to retrieve correction factors that can be used in conjunction with B-station recordings to obtain equivalent free field motions. Corrections could be either correction on recorded ground motions (represented in the time or frequency domain) or corrections directly on response spectra which is the typical GMM-representation of ground motion hazard.

Simple models for kinematic interaction are developed to transform free field ground motions to foundation input motions (FIM). The FIM is the theoretical motion of the foundation slab if the foundation and super structure had no mass. The FIM is generally considered to be a more appropriate motion for structural response analysis than is the free field motion. It should be noted that next to kinematic effects also system response effects including the response of the building superstructure will affect the recorded B-station motions. In order to capture this as well one would need to extend the models as described in (Witteveen+Bos, 2019b) to include incoherent spatially variable wave fields. This can be done but is not part of the study presented in this report.

Kinematic interaction effects, Id Est variations between free field ground motions and foundation motions, for shallow foundations could be covered based on simple models. For piled foundations such simple models are not applicable, and one would need to set up more elaborate models to capture all relevant aspects. In the present study the simple models are applied to all B-station buildings, in order to trace if the correction which would apply for the shallow foundation system captures the observed trends for piled foundations as well. It should be recognized that based on the available information BUHZ has piled foundations and for several others the exact foundation type is unknown.

The basis of the present study are FAS and SA ratio comparisons between close by B- and G-station couples in Groningen. The stations network is illustrated by figure 1.1. The couples of B- and G-stations considered are: BAPP-G670, BFB2-G450, BGAR-G610, BHAR-G390, BHKS-G290, BLOP-G180, BMD2-G130, BOWW-G190, BSTD-G220, BUHZ-G040, BWIN-G230, BWIR-G230, BWSE-G180, BZN1-G140, BZN2-G140.

Figure 1.1 Overview of stations. Brown coloured stations are G-stations downhole arrays with an accelerometer at ground surface and geophones at 50, 100, 150 and 200 m depth. Green coloured stations are the B-stations positioned in buildings at foundation level

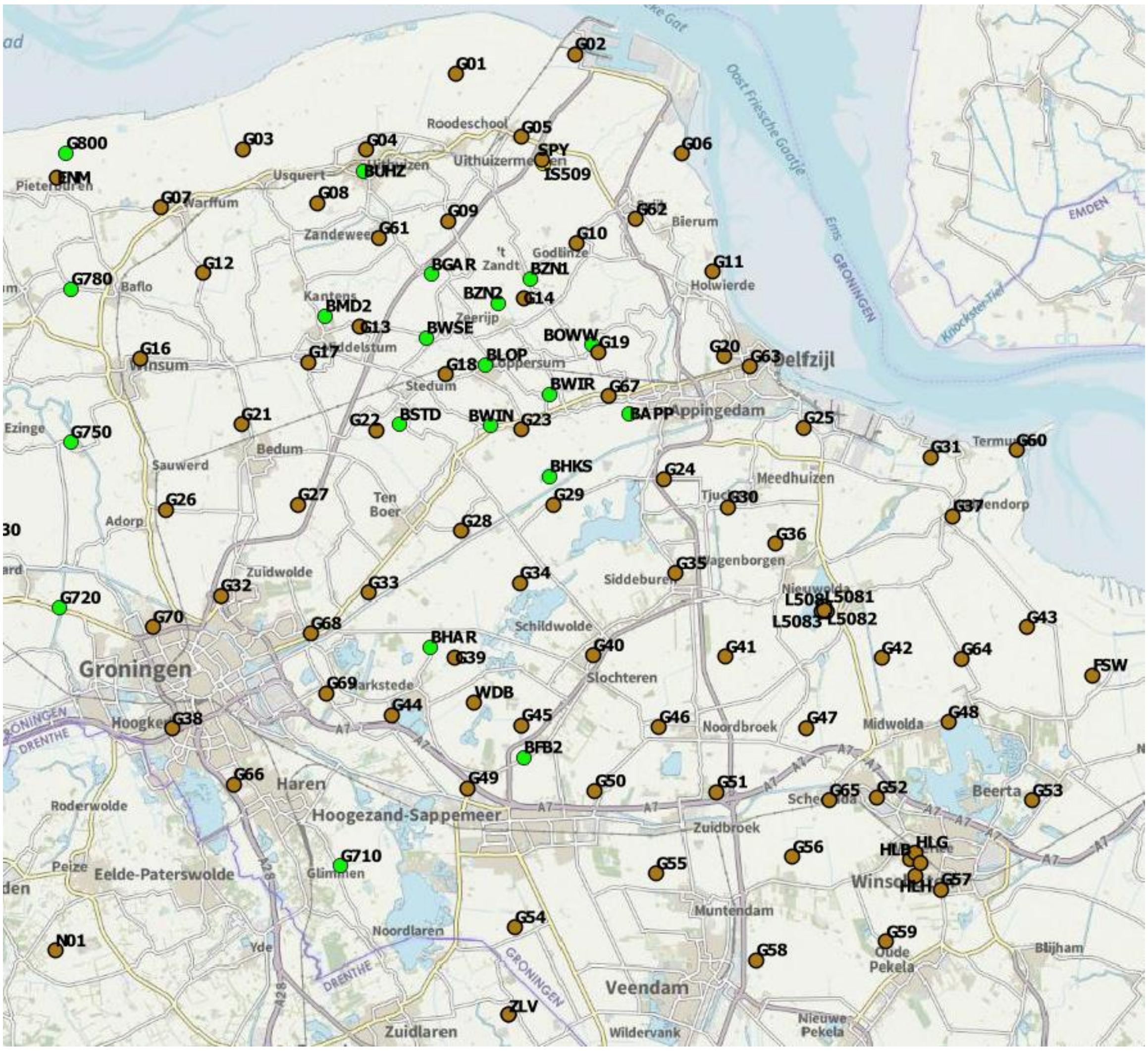

## 1.3 Document structure

Chapter 1 gives and introduction to and outline of the present document. In chapter 2 the research methodology is explained. Chapter 3 gives the analysis results. Chapter 4 reports conclusions and recommendations. References used are listed in chapter 5.

# 2

## RESEARCH METHODOLOGY

### 2.1 Methodology outline

Codes like NIST (NEHRP Consultants Joint Venture, 2012) and FEMA 440 (NEHRP, 2005) provide correction factors represented as ratio to response spectra (RRS) that may be applied to calculate foundation input motion response spectra from free field ground motion response spectra. Two correction factors are distinguished;

1 RRSbsa, a correction factor for base slab averaging effects. and
2 RRSemb, a correction factor for embedment effects.

Although the RRS may seem the most straight forward tool to calculated modified B-station records, these cannot be applied directly to Groningen field. The RRS provided by codes are simplified formulations, derived based on analytical-empirical formulations that calculated such effect in the frequency domain. Factors of influence in these formulation are frequency content of the ground motion, shear wave velocities of the soil and angle of incidence of the incoming waves. These factors are all not present in the RRS factors and therefore the specific situation of the Groningen B-stations cannot be directly captured by these RRS.

For this reason the present study aims to substantiate correction factors based on the analytical-empirical formulations ( (Veletsos & Prasad, Seismic interaction of structures and soils: stochastic approach, 1989) ( , 1997) ( 2003) ( , 1977)) that form the basis of the RRS in codes (hereafter we refer to these as the Veletsos & Prasad method). In order to do so FEMA 440 suggests the following approach which has been followed in the present study as well:

1 Calculate the Fourier transform of the time histories.
2 Multiply the Fourier transform by the amplitude of the transfer function.
3 Use the modified amplitudes along with the phase angles of the original motions and perform inverse Fourier transform to estimate the modified time histories.
4 If needed, a modified response spectrum that accounts for kinematic effects could be calculated from the modified time histories.

Subsequently it has been investigated if modifications to RRS as presented in NIST (NEHRP Consultants Joint Venture, 2012) and FEMA 440 (NEHRP, 2005) are necessary in order to make them applicable for Groningen.

The factors of influence taken into account in the present study are summarized in figure 2.1. The objective of the present study is to identify if consistency between B- and G-station recordings for the selected couples increases if distance effects, site response effects and kinematic effects (consisting of base slab averaging effects and embedment effects) are taken into account according to correct recorded ground motions as described above.

Figure 2.1 Graphical representation of effects considered

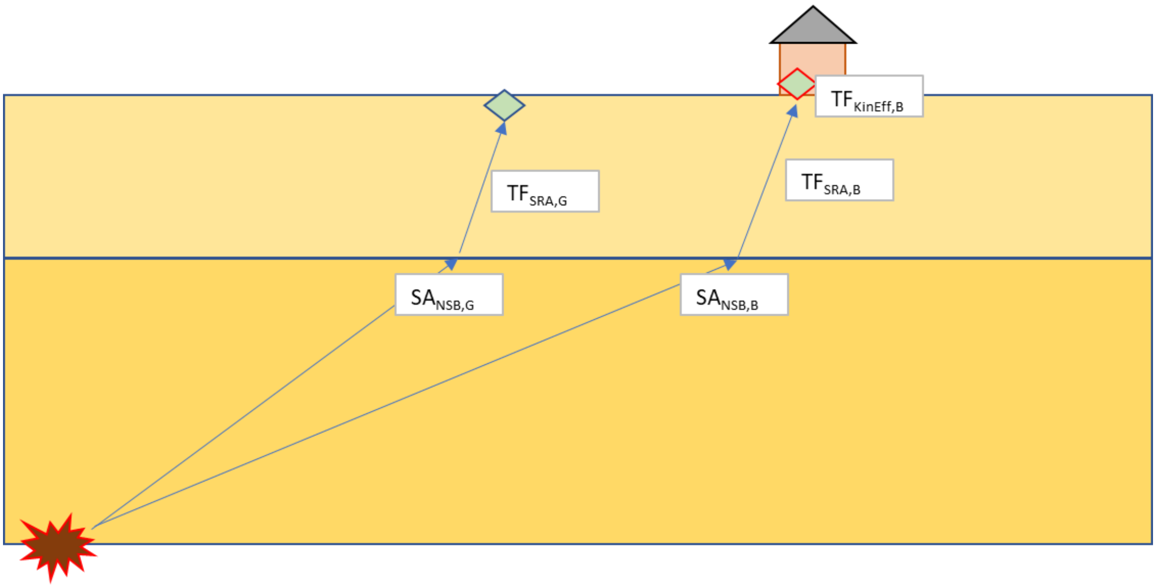


Consistency is defined herein as FAS-ratios and spectral acceleration ratios close to 1.0. Uncorrected ratios are compared with corrected ratios in which the corrections are made according to the following formulas:

For FAS:

$$FAS_{B,uncorrected}(\omega) = abs(\ FFT\ (\ a_{B,uncorrected}(t))$$

$$FAS_G(\omega) = abs(\ FFT\ (\ a_G(t))$$

$$FAS\ ratio(\omega) = \frac{FAS_{B,uncorrected}(\omega)}{FAS_G(\omega)}$$

$$FAS_{B,corrected}(\omega) = \frac{FAS_{B,uncorrected}(\omega)}{\frac{SA_{B,NSB}(0.01s)}{SA_{G,NSB}(0.01s)} * \frac{TF_{B,SRA}(\omega)}{TF_{G,SRA}(\omega)} * TF_{B,KinEff}}$$

$$FAS\ ratio = \frac{FAS_{B,corrected}(\omega)}{FAS_G(\omega)}$$

For SA:

$$SA_{B,uncorrected}(T) = Response\ spectrum(\ a_{B,uncorrected}(t)\ )$$

$$SA_G(T) = Response\ spectrum(\ a_G(t)\ )$$

$$SA\ ratio(T) = \frac{SA_{B,uncorrected}(T)}{SA_G(T)}$$

$$a_{B,corrected} = IFFT\ (\ FAS_{B,corrected}(\omega))$$

$$SA_{B,corrected}(T) = Response\ spectrum(\ a_{B,corrected}(t)\ )$$

$$SA\ ratio(T) = \frac{SA_{B,corrected}(T)}{SA_G(T)}$$

Where NSB refers to North Sea supergroup and SRA to site response analysis. In which, following the procedure suggested by FEMA 440, for the IFFT the TF are assumed to only operate on FAS amplitude and the phase information from the original signal is retained. This is a simplified procedure proposed by FEMA 440 for the calculation of the SA of foundation input motions.

## 2.2 Distance effects

Given the grid of B-stations and G-stations the couples that result from selection of closest B-stations and G-stations have interstation distances ranging from 420 to 2,600 m. For events at relatively short distance from the couple of stations, a significant difference of ground motion amplitudes should be expected. For couples of stations that have recorded many events, and which are located in the centre of the field one may expect that in the FAS- and SA-ratio presentation the distance effect cancels out. However, this is possibly not valid for couples of stations that have recorded a few events only, or for couples of stations at edge of the field. These latter group may show a non-unity ratio if either the B-station or G-station is located more closely to recorded events epicentres.

The exact effect of distance on amplitude per frequency bin of the FFT is unknown and beyond the scope of the present study. A straight forward correction has been implemented, by linear scaling of the record by a constant factor per event-station combination based on mean GMM v5 (Bommer , 2018) predicted peak ground acceleration at NS_B (SA(T=0.01s)), as follows:

$$Correction\ of\ ratio\ for\ distance = \frac{SA_{NSB,B}\left(M_w,\ R_{epi,B},\ T = 0.01s\right)}{SA_{NSB,G}\left(M_w,\ R_{epi,G},\ T = 0.01s\right)}$$

## 2.3 Site response effects

Local soil conditions will typically vary between the locations of couples of B-stations and G-stations. A couple may be either located within the same zone or in different zones of the GMM. But even within a zone, variations may cause significant differences between ground response transfer functions $TF_{SRA}$ of two locations. The location of the stations in conjunction with the GMM v5 zonation is shown in figure 2.2. This has been taken into account for couples where a high resolution soil profile characterisation was available for both the B-station and the G-station (BAPP-G670, BFB2-G450, BGAR-G610, BOWW-G190, BSTD-G220, BWIN-G230, BWIR-G230, BZN1-G140 and BZN2-G140).

Using the GMM v5 STRATA-realisations for the voxel-stack locations of the B-stations and G-stations a site response transfer function in the frequency domain has been calculated. The ratio of the transfer functions of two stations represents the predicted effect of different soil conditions on the surface ground motion. It has been evaluated if the transfer function ratios could (partially) explain observed differences in FAS-ratios of B- over G-station recordings. The transfer function ratio has been defined as follows:

$$FAS_{B,corrected}(\omega) = \frac{FAS_{B,uncorrected}(\omega)}{\frac{TF_{B,SRA}(\omega)}{TF_{G,SRA}(\omega)}}$$

Figure 2.2 Station couples location with GMM v5 zonation

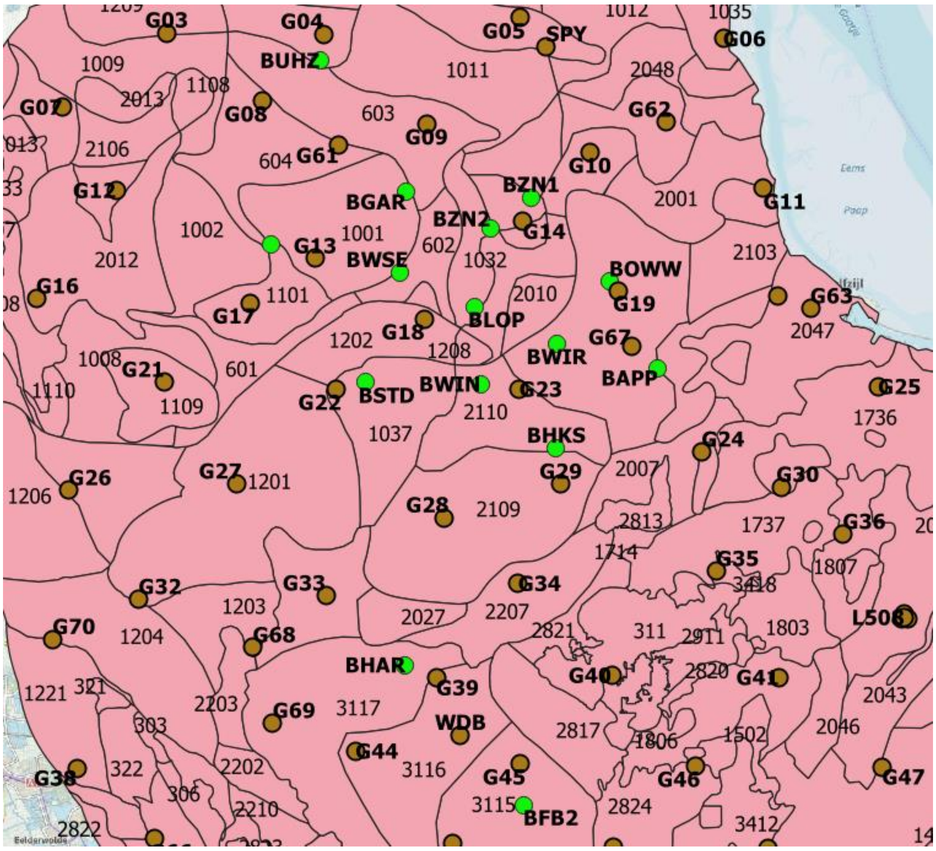


## 2.4 Kinematic interaction damping effects

Kinematic interaction results from the presence of stiff foundation elements on or in soil. This causes foundation motions to deviate from free-field motions as a result of base slab averaging and embedment effects. The base slab averaging effect can be visualized by recognizing that the motion that would have occurred in the absence of the structure within and below the footprint of the building is spatially variable. Placement of a foundation slab across these variable motions produces an averaging effect in which the foundation motion is less than the localized maxima that would have occurred in the free-field. The embedment effect is simply associated with the reduction of ground motion that tends to occur with depth in a soil deposit. In this section the description of correction models for base slab averaging is separated from the embedment effects. Both models are combined to obtain transfer functions for ground motions due to kinematic interaction effects.

### 2.4.1 Base slab averaging

The models adopted to correct ground motions for base slab averaging effects are developed by Veletsos and Prasad ( (Veletsos & Prasad, 1989), (Veletsos, Prasad, & Wu, 1997)) and valuable additions are added by , 2003) and , 1977). FEMA 440 provides a concise outline of the framework of these models. For details about the models one is referred to the Veletsos papers.

Base slab averaging covers two phenomena, being the effects of incoherency and oblique incidence of wave arrivals on the resulting foundation motion. As a result, base slab translational motions are typically reduced (this is the effect observed in (Seister, 2019) which has initiated the present study) and rotational motions are introduced. In the present study, the introduction of rotational motions is not considered. This is because validation of such effects based on recordings is complicated due to the large interstation distance.

Furthermore, one would need to include a detailed superstructure model as well. Given the amplitudes of possible resulting rotational motions relative to amplitude reduction of translational motions, this limitation is considered acceptable.

According to Veletsos and FEMA 440 the lateral transfer function is predominantly a function of total foundation area and not very sensitive to the ratio of foundation dimensions. Moreover, orientation of B- and G-stations relative to the epicentre differs for every event. For this reason, the transfer functions have been applied to the geomean horizontal ground motions based on the effective foundation size. This is considered appropriate given the objective of the present study and the inherent variations that are observed from the spatial separation of B- and G-stations that are compared.

Other parameters that enter the base slab averaging transfer function are ground motion incoherency parameter κ and angle of oblique incidence α. Kim and Stewart (Kim & Stewart, 2003) analysed the level of κ based on case history data and concluded upon an expression that calculates κ as a function of the soil shear wave velocity. FEMA 440 suggests that according to (Elsabee & Morray, 1977) the average shear wave velocity over depth equal to the effective foundation size results appropriate κ values. The values for κ proposed by are adopted in FEMA 440 and are used in the present study as well. The shear wave velocity profiles are defined in accordance with the GMM v5 voxel stack profiles at the B-station locations (Bommer , 2018). Angle of oblique incidence α is estimated in the present study using Snell's law as function of epicentral distance and the generalized typical deep soil shear wave velocity profile in the region in accordance with (KNMI, 2013) 2017). A simplified model with five layers has been used for the purpose of the present study, as illustrate by figure 2.3 where the soil shear wave velocities are assumed to range from 2,200 m/s to 200 m/s. This gives the angle to distance relation as presented in figure 2.4.

Figure 2.3 Generalized simplified 5-layer soil shear wave velocity profile for angle of oblique incidence calculation

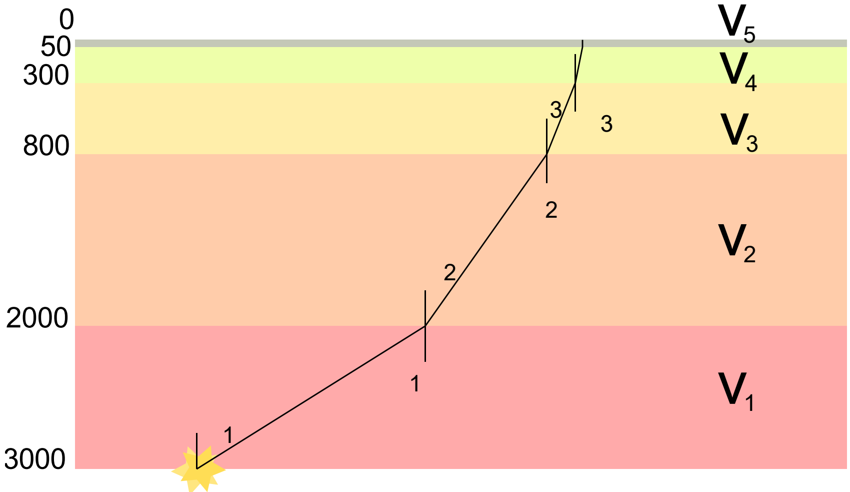

Figure 2.4 Simplified relation between distance to epicentre and angle of oblique incidence

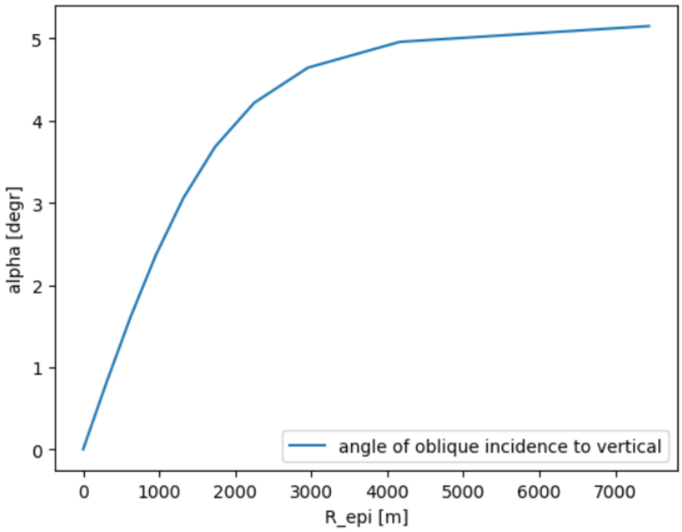


Base slab averaging effects are frequency dependent and tend to become more significant for higher frequencies, which could be explained by the increased effective size of a foundation relative to seismic wave lengths for high frequencies. The frequency dependency of the lateral foundation motion transfer function is illustrated by figure 2.5. Stronger events typically contain more frequency content in the lower frequency range and therefore will show less reduction of B-station motion compared to G-station motion.

Figure 2.5 Transfer function for translational ground motions due to base slab averaging effects, left: dependency on equivalent foundation size, right: dependency on shear wave velocity

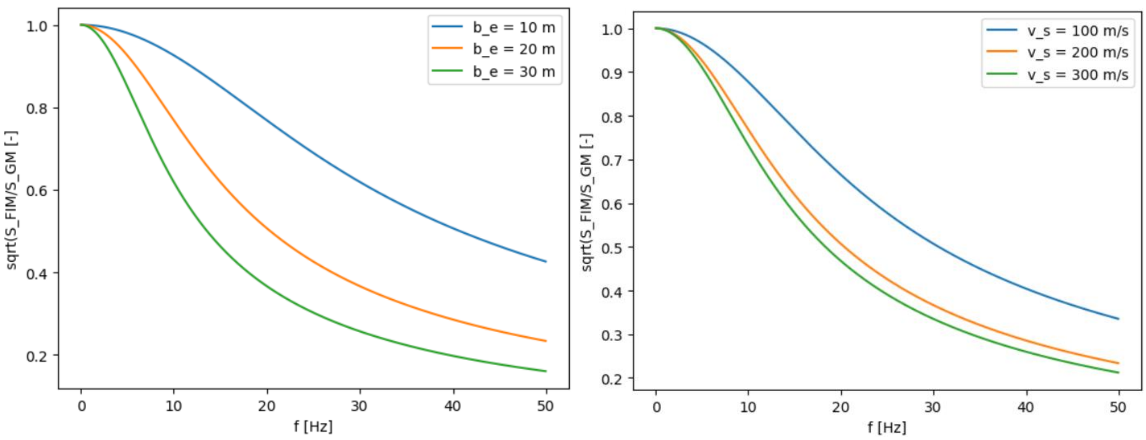


In addition to the calculation based on transfer functions (as described above), corrections for B-station recorded ground motions are, for comparison reasons, also calculated using the simplified $RRS_{bsa}$ formula provided by FEMA 440. Preliminary calculation results indicated that the RRS relations that are proposed by FEMA 440 do not apply to Groningen cases. This is reasonable because where tectonic earthquakes may have their energy concentrated at frequencies up to 5 Hz, for Groningen we observe energy content in frequencies ranging from 8 to 10 Hz for higher magnitude events and even above 10 Hz for smaller magnitude events. In addition, the shallow subsurface in Groningen shows shear wave velocities typically around 200 m/s, where across the world 400 m/s is a more common value. With wave lengths being calculated as $\lambda = v_s/f$, a wavelength ratio of about 3.2 would apply for typical Groningen conditions. Since foundation dimensions relative to seismic wave lengths are a parameter for kinematic effects, this should be accounted for. The more elaborate framework by Veletsos takes this into account, but in the RRS-factors that are proposed by FEMA 440 for direct modification of response spectrum ordinates this is not done. Therefore, we have applied this wavelength correction factor to the effective foundation size in the RRS-formula, in order to obtain more realistic results. This modifies the FEMA 440 RRS relation into:

$$RRS_{bsa} = 1 - \frac{1}{14100} * \left(2 * \frac{\frac{b_e}{0.3125*0.3048}}{T}\right)^{1.2} \quad \text{for } T > \frac{1}{f_l}$$
$$RRS_{bsa} = 1 - \frac{1}{14100} * \left(2 * \frac{b_e}{0.3125*0.3048} * f_l\right)^{1.2} \quad \text{for } T \leq \frac{1}{f_l}$$

Where $b_e$ is effective foundation half-length in m, T is period in seconds and $f_l$ is the limit frequency typically around 5 Hz.

Calculations reported in (Witteveen+Bos, 2019b) indicate that no significant modification of the free field ground motion applies for the G-station surface accelerometers. Base slab averaging formulas from (NEHRP, 2005), (Veletsos & Prasad, 1989) (Veletsos, Prasad, & Wu, 1997) confirm this conclusion. Applying the base slab averaging framework for a 2 x 1 m plate, as would apply to G-stations, results transfer functions values effectively equal to unity.

### 2.4.2 Foundation embedment

FEMA 440 provides expressions to calculate foundation input motions from ground motions as a function of foundation embedment depth. According to FEMA 440 the same expression applies for the frequency domain transfer function and for the ratio of response spectrum ($RRS_{emb}$). These relations are adopted in the present study:

$$RRS_{emb} = cos\left(\frac{2*\pi*d_{emb}}{T*v_{s,r}}\right)^{1.2} \quad \text{for } T > \frac{1}{f_l}$$
$$RRS_{emb} = cos\left(\frac{2*\pi*d_{emb}*f_l}{v_{s,r}}\right)^{1.2} \quad \text{for } T \leq \frac{1}{f_l}$$

Where $d_{emb}$ is foundation embedment depth in m, T is period in seconds, $v_{s,r}$ is average soil shear wave velocity over the depth equal to the effective foundation size and $f_l$ is limit frequency typically around 5 Hz.

As noted in section 2.1 the simplified framework for modification of ground motions into foundation input motions considered in the present study does strictly not apply to piled foundations. The application of the present framework to piled B-station buildings has been briefly tested, by considering as foundation depth the pile lengths. It is concluded that this indeed result a significant overshoot in corrections of both FAS and response spectra compared to the close G-stations. Accordingly, for buildings that have piled foundations or an unknown foundation type, the approximated embedment depth of foundation beams/strips or eventually its basement has been taken into account as embedment depth. This depth is typically limited and consequently only for buildings that have a basement. The embedment correction turns out to be significant.

# 3

# RESULTS

## 3.1 Presentation of results

Calculation results are presented in this chapter by means of:
- FAS ratios of the B-station record over the coupled G-station record.
- Spectral acceleration ratios of the B-station record over the coupled G-station record.
- Acceleration response spectra of the original B- and G-station records and the modified B-station records using both the full Veletsos TF-based method and the generalized FEMA 440 RRS-based method.

Preliminary calculation results indicated that ratios of B- over G-station records in the frequency domain (FAS) do not only tend to show a decreasing trend with frequency, but also gradual fluctuations causing clear peaks and troughs. It has been investigated if this could be quantitatively corrected based on the transfer functions that were extracted from STRATA-realizations of the corresponding voxel stacks, which were used for the development of the GMM v5. Accordingly, calculation results that include a correction and results that do not include a correction for site response effects, are presented separately.

To this extend, three sets of results are included as appendices of this report:
- Appendix I: reference results (no modification of B-station records).
- Appendix II: calculation results - B-station records modified, excluding ground response correction.
- Appendix III: calculation results - B-station records modified, including ground response correction.

## 3.2 Reference results

Uncorrected B-station to G-station ground motion ratio plots were used as reference results in the present study. FAS and response spectra have been calculated from processed ground motions. Processing steps that were conducted are detrending, high-pass filtering with a fourth order Butterworth filter at 0.7 Hz and notch filtering to remove the peak in records around 50 Hz, following from the utility frequency of the electric power grid. These results are shown in appendix I.

Comparison of the original FAS and SA ratios yields the following observations:
- Small and/or light weight B-station buildings like BOWW, BGAR, BLOP were expected to not show clear kinematic interaction effects. The processed data confirms this.
- Large and/or massive B-station buildings like BFB2, BHAR, BMD2, BSTD, BUHZ and BZN1 were expected to show clear kinematic interaction effects. The processed data confirms this. However, there are also stations located in large buildings (at least large in plan dimensions), like BZN2, that hardly show ratios lower than 1.0. This could probably be explained by the non-rigidity of the foundation system for this building, but there is no model data available to proof this hypothesis.
- BWIN and BWIR are both compared to the same, closest G-station: G230. A very similar trend in both FAS and SA ratio plots are observed for these two couples, not only with respect to the absolute decay towards higher frequencies but also the peaks and troughs over the total frequency range. This raises the question to what extend not only the building typologies are similar, but also to what extend the site

conditions at BWIN and BWIR are comparible. This makes these cases particularly interesting for further investigation.
- For frequencies beyond 15 Hz, an interesting increasing trend in the FAS- and SA-ratios is observed with increasing frequency. BHAR and BUHZ are the cases that show this effect the clearest.
- BGAR - G610 seem to show a distance effect which is reasonable, given the location of the stations relative to the recorded event epicentres.

## 3.3 Results B-station records modified, without ground response correction

### 3.3.1 Summary table

Based on comparison of the original FAS-ratios, SA-ratios and absolute SA-ordinates, it has been judged if signal modification following the methods introduced in chapter 2 has been applied successfully. This evaluation is summarized in table 3.1.

Table 3.1 Summary of quality of records correction (without site response correction)

| B-station | G-station | Quality of FAS correction | Quality of SA-correction method Veletsos FAS TF | Quality of SA-correction method FEM 440 SA RRS |
|---|---|---|---|---|
| BAPP | G67 | good | mediocre, limited impact | mediocre, limited impact |
| BFB2 | G45 | good, except f >15 Hz | good, to high ratios high freq | good |
| BGAR | G61 | good | good | good |
| BHAR | G39 | poor | poor, G-station higher SA | poor, G-station higher SA |
| BHKS | G29 | good | limited impact | limited impact |
| BLOP | G18 | limited impact | limited impact | limited impact |
| BMD2 | G13 | mediocre, overshoot f > 15 Hz | mediocre, overshoot f > 15 Hz | good |
| BOWW | G19 | limited impact | limited impact | limited impact |
| BSTD | G22 | mediocre | mediocre | good |
| BUHZ | G04 | poor | poor | poor |
| BWIN | G23 | good | poor, G-station freq content around 8-9 Hz seems dominant | poor, G-station freq content around 8-9 Hz seems dominant |
| BWIR | G23 | good | poor, G-station freq content around 8-9 Hz seems dominant | poor, G-station freq content around 8-9 Hz seems dominant |
| BWSE | G18 | good, limited impact | good, limited impact | good, limited impact |
| BZN1 | G14 | good, offset for low frequencies | good for low periods | good for low periods |
| BZN2 | G14 | mediocre | mediocre | mediocre |

For the total set of calculation results, one is referred to appendix II. Figure 3.1 shows two examples of the FAS-representation of records from B-stations (top) and the corrected FAS using the Veletsos method (bottom), where the correction is concluded to be successful. It can be seen that the drift to values below unity towards the higher frequencies is successfully corrected if the FAS of the B-station records are divided by the transfer functions introduced in section 2.1. Cases for which the correction is concluded to be unsuccessful, will be discussed in more detail in the following paragraphs.

Figure 3.1 FAS-ratios B over G original (top) and modified using Veletsos transfer functions (bottom) for examples of cases that show good results

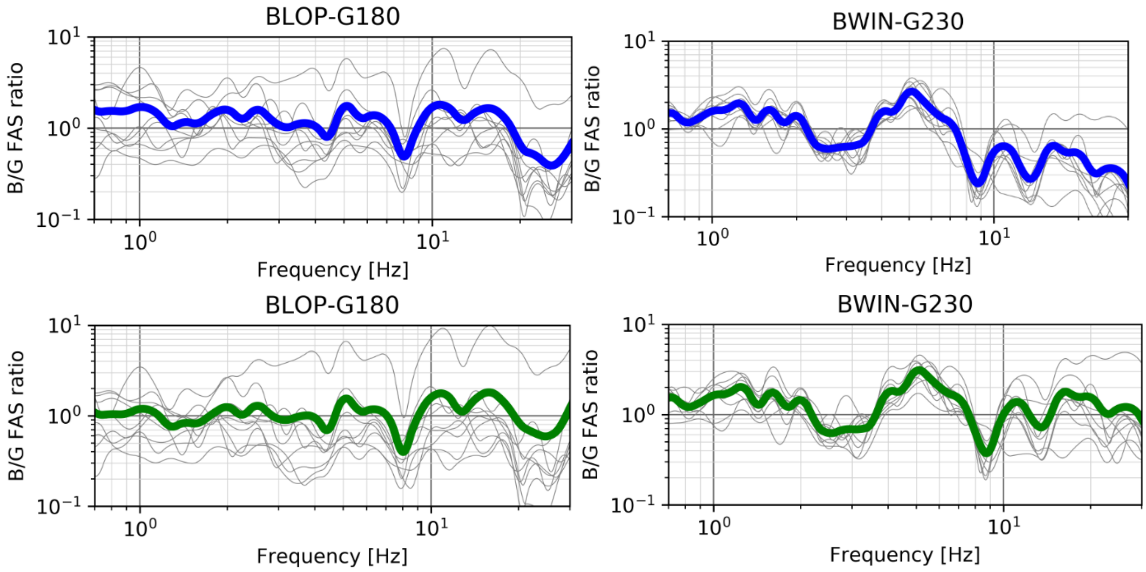


## 3.3.2 Evaluations

This section of the report summarized the obtained results by showing a sub selection of the total set of results and addressing specific observations.

### Trends in FAS-representation

FAS is concluded to be a very sensitive representation in all cases. Inherent randomness in ground motions is clearly reflected in FAS and therefore also in FAS-ratios. Interestingly, there are cases like BFB2-G450, BHAR-G390 and BLOP-G180 for which the FAS-ratios are fluctuating, but a clear consistent trend of peaks and troughs is observed for different events. Other couples of stations, like BSTD-G220, BWIN-G230, BWIR-G230 show a very consistent trend over the frequency range. An example for both groups is illustrated by figure 3.2. For the latter group of couples, specific attention has been paid to evaluation if differences in ground response provides an explanation.

Figure 3.2 Consistency of FAS-ratio for different events

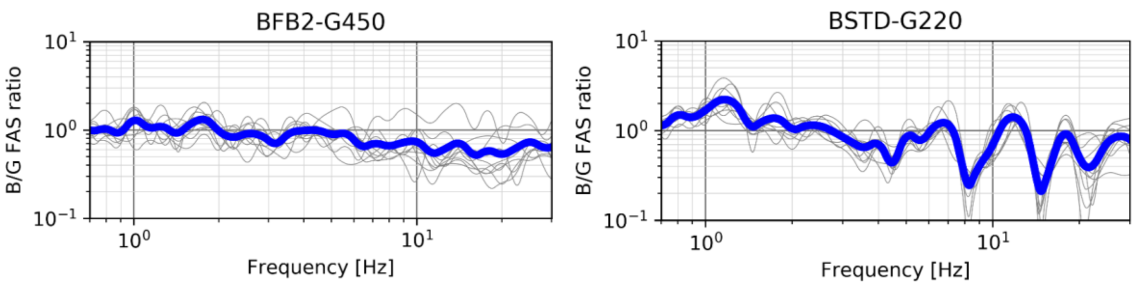


### Sensitivity obtained from response spectra and SA-ratio plots

Moreover, by examining the records separately, we observed that one event resulted in a ground motion with three times higher intensity (PGA and spectral accelerations) compared to the rest of the ground motions recorded by the same stations. The local response of both B- and G-station for this event, using linear averaging of response spectra, becomes very dominant in the calculated average SA-plot (top left figure of figure 3.3). Meanwhile, we do not observe this very clearly from the SA-ratio plots which linearly average ratios instead of absolute values.

Figure 3.3 Case BMD2-G130, sensitivity of SA-corrections

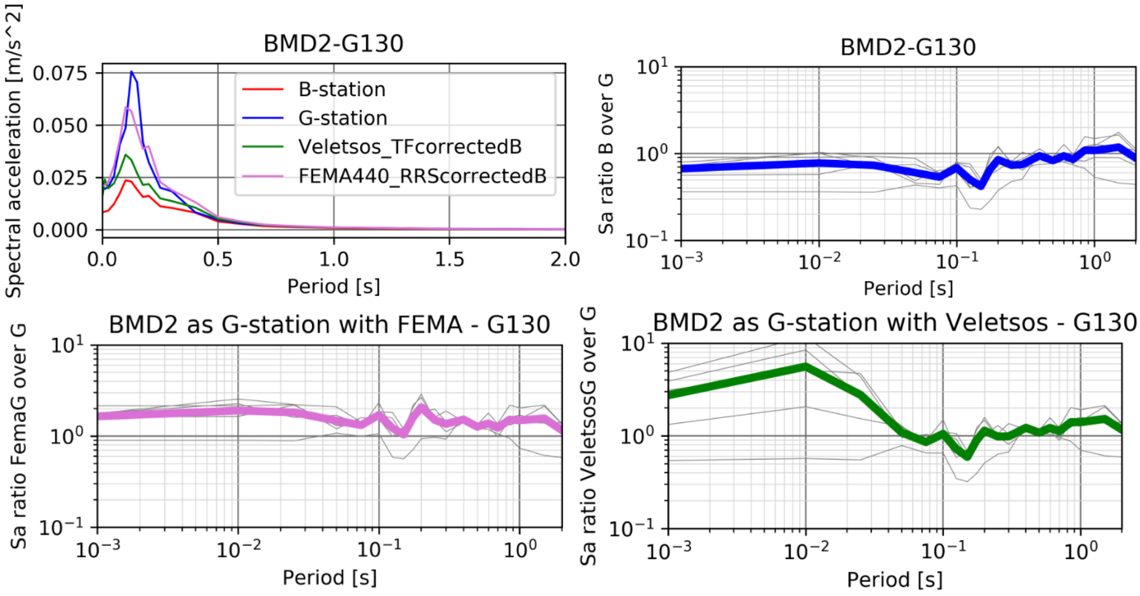


## Bump in SA-ratio plots after correction

B-station over G-station spectra acceleration ratio plots for a number of stations are shown in figure 3.4. For calculation results of other stations, one is referred to appendix II. Both the Veletsos method and the FEMA 440 method result in a satisfactory correction to transform B-station motions into ground motions that are similar to the ground motions recorded by the coupled G-stations. The ratios following from the corrected B-station motions are close to unity for most stations over the entire period range (appendix II), which is clearly different from the reference results (appendix I). The total set of stations also shows station couples for which calculated ratios deviate more from unity. Further analysis could possibly indicate what has caused these station specific deviations. Apart from this, one may notice a bump in the SA-ratio plots. This bump seems to be consistent with the resonance frequencies of the soil-foundation-building systems as reported in (Witteveen+Bos, 2019b), being about 2 Hz, 4 Hz, 10 Hz and 0.15 Hz for BAPP, BFB2, BOWW and BSTD respectively. Possibly this applies to other stations as well, but for those cases, the system resonance characteristics are not further analysed.

Figure 3.4 SA-ratios of FEMA 440 RRS based modification of B-station record over G-station record

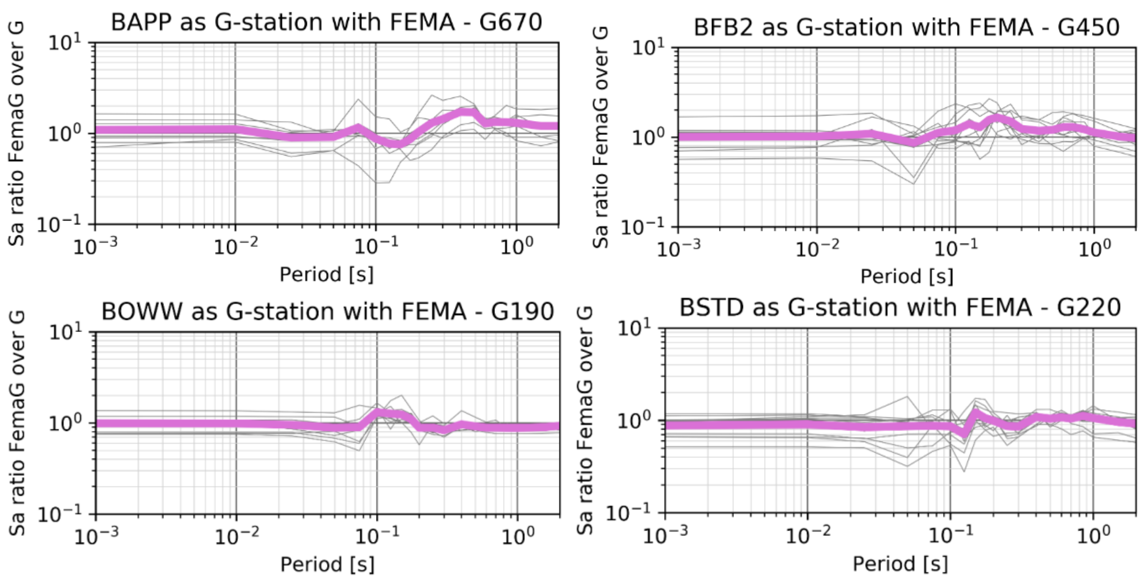

### High SA-ratios for frequencies beyond 15 Hz

From the calculation results of some station recordings (BFB2, BHAR, BMD2, BUHZ, BZN2), a decent correction in the frequency range up to 15 Hz is observed, but for higher frequencies the modification following the Veletsos framework is not appropriate. This is illustrated by figure 3.5 and it is not considered to be directly related to the Veletsos transfer functions. This is because the frequency-dependent correction factor in this high frequency range is decreasing gradually, as illustrated by figure 2.5.

Figure 3.5 FAS-ratios B over G original (top) and modified using Veletsos transfer functions (bottom) for examples of cases that show poor results

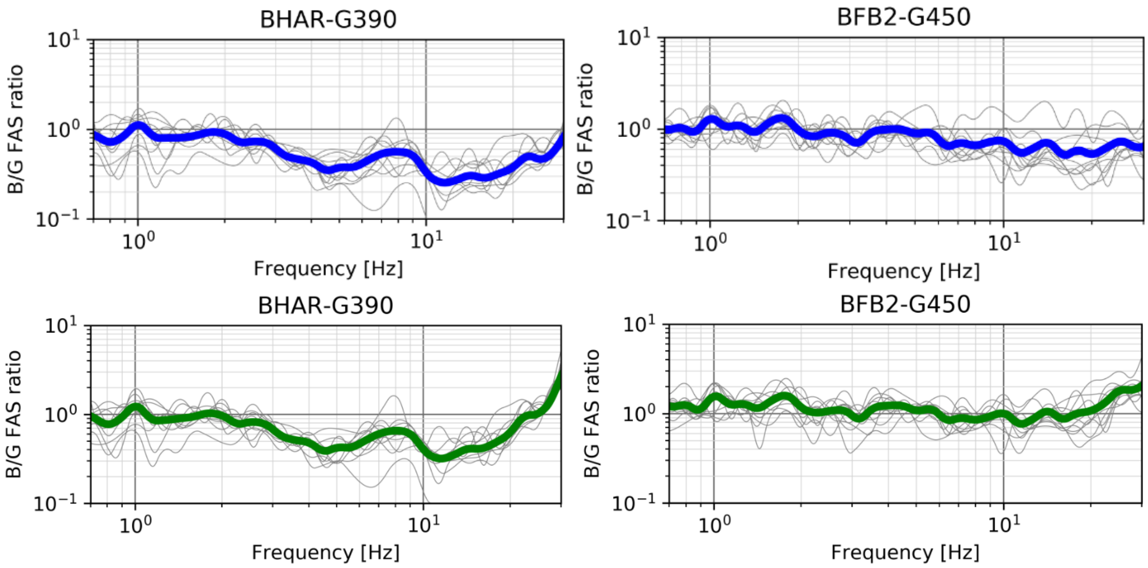


Instead, the observed effect seems to be caused by the characteristic of the original B-station recordings. For the stations listed above, the uncorrected ratio shows already a clear increasing trend. No available literature could justify this in relation to kinematic interaction. An explanation could be the ground motion characteristic in this frequency range. In accordance with the time-frequency representation of observed ground motions (Witteveen+Bos, 2019a), ground motions mainly show the >15 Hz frequency content during the early part of the record. Figure 3.6 to figure 3.9 illustrate this by means of time-frequency representations of ground motions recorded by couple BFB2 - G450 for the relatively weak Froombosch event and couple BLOP - G180 for the relatively strong Zeerijp event. In the early stage of ground motion, P-waves arrive, and ground motions are dominated by P-waves. P-waves have much longer wave lengths compared to S-waves and accordingly the corresponding ground motions will be less affected by kinematic interaction effects. Possibly this forms an explanation, but this hypothesis has not been further substantiated by numerical simulations. Another possible explanation could be related to non-rigidity of the foundation system, not being a rigid plate. This implies that the base slab averaging effect is overestimated in this frequency range. However, this could not be proven based on the available data and requires further investigation.

Figure 3.6 Record event: Froombosch 2016, station: BFB2

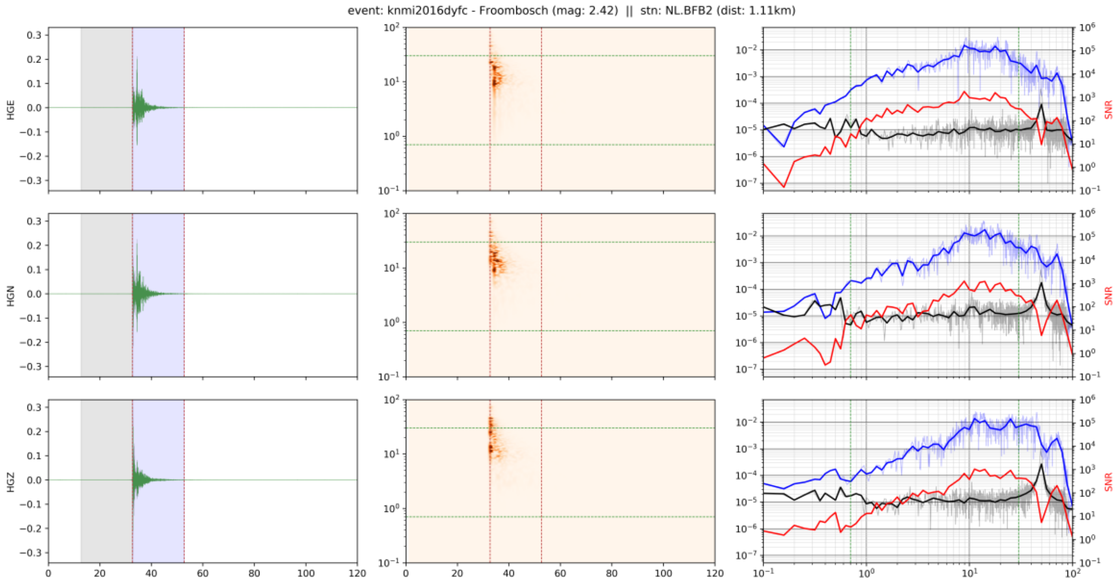


Figure 3.7 Record event: Froombosch 2016, station: G450

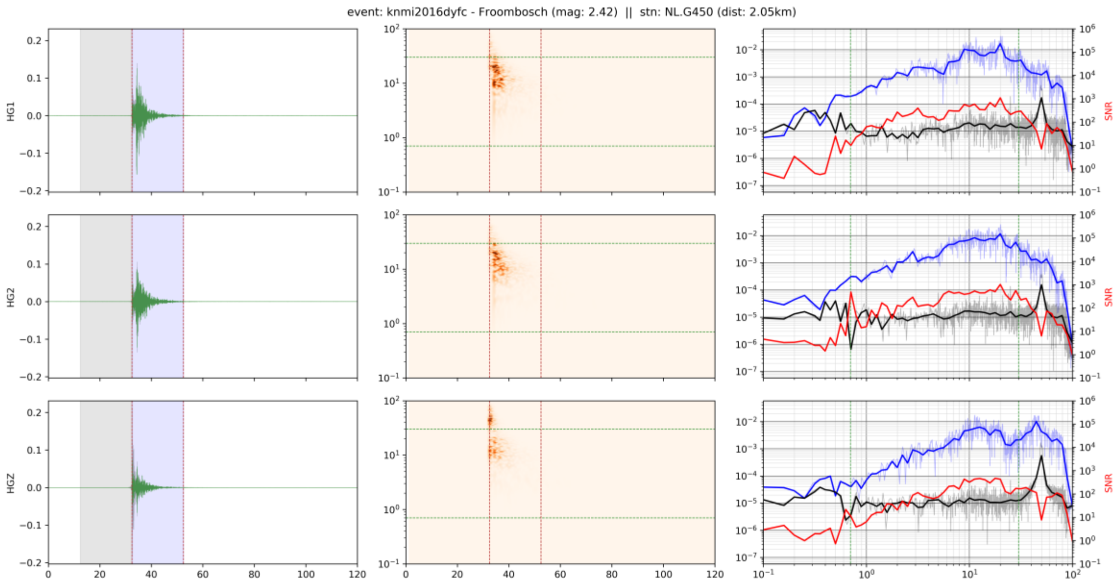

Figure 3.8 Record event: Zeerijp 2018, station: BLOP

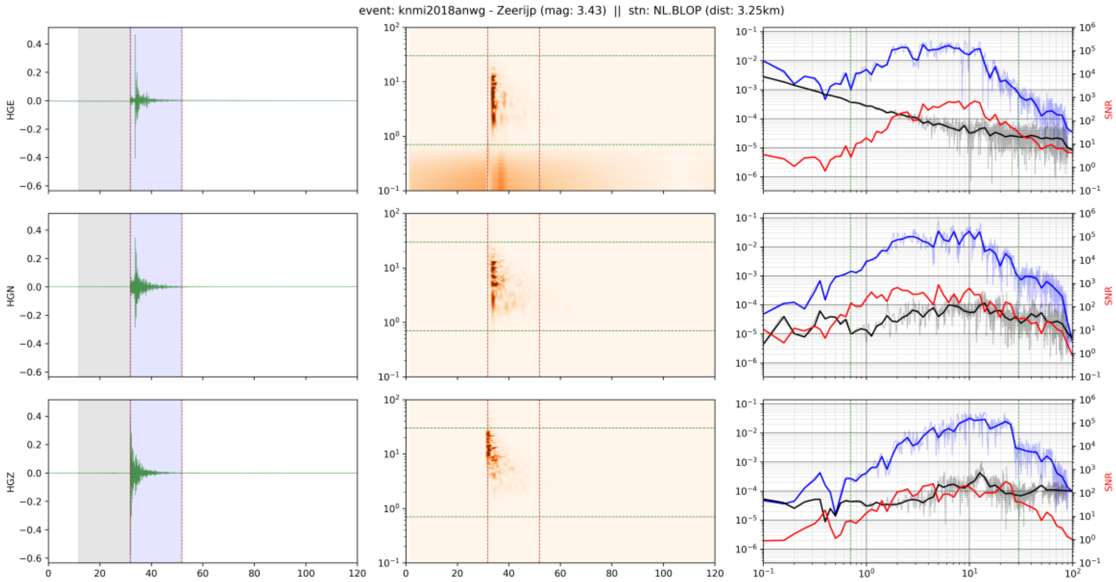


Figure 3.9 Record event: Zeerijp 2018, station: G180

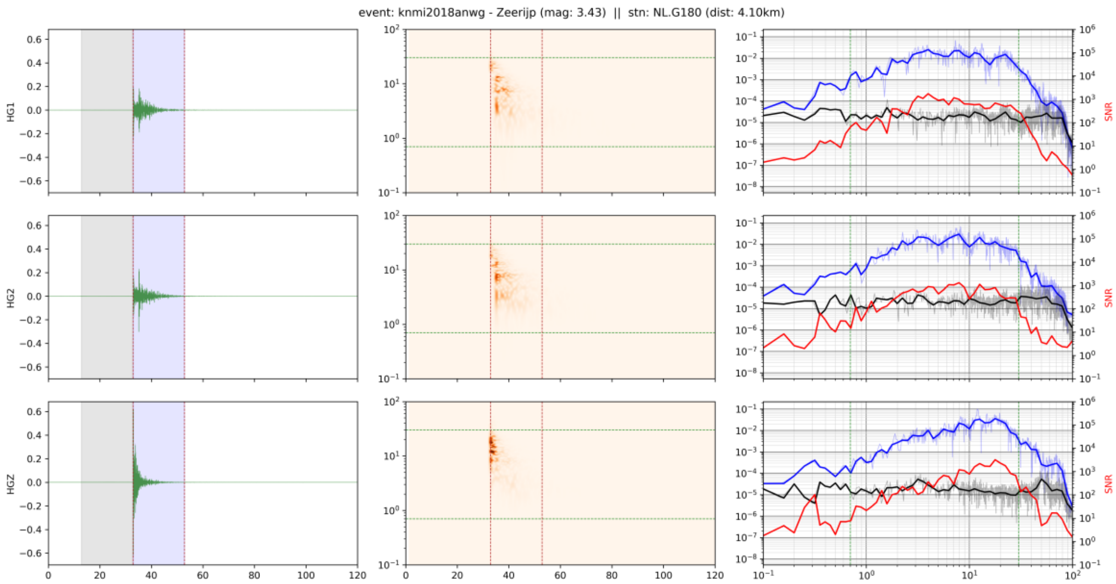


## 3.4 Results B-station records modified, with ground response correction

This section discusses calculation results including a correction to account for differences in ground response. The aim of these additional evaluations is to investigate if ground response could explain deviations between B- and G-station records as reported in 3.3. Such additional evaluations are only conducted for couples of stations for which an SCPT is available for both stations. If not, differences in ground response effects among the stations are simply too uncertain to have added value in the analyses.

### 3.4.1 Ground response transfer function ratios

Ground response has been calculated for B- and G-station locations. The GMM v5 voxel stack realisations at the locations of coupled B- and G-stations are used as a starting point (Bommer , 2018). The GMM v5 voxel stacks of the G-stations have been adjusted in accordance with SCPT-data (that have become available per May 2019) over the penetration depth of the SCPT. Subsequently, the response functions are calculated by STRATA.

In line with the Veletsos method, which accounts for kinematic effects by means of transfer functions operating on the Fourier transform of a record, a ground response correction could also be covered by a transfer function ($TF_{SRA}$). The ratio of the site response analysis transfer function of the B-station soil profile over the G-station profile should theoretically apply to the ratio of B- over G-station FAS. Calculated ratios $TR_{SRA,B}/TF_{SRA,G}$ are shown in figure 3.10.

Likewise, for SA-ratios of B- over G-station records, the site response amplification function (AF) as developed for the GMM v5 is supposed to be correlated to the calculated SA-ratio of B- over G-stations. Unlike the transfer functions for FAS-correction, operators on spectral accelerations are equivalent functions to cover the mechanism (ground response or kinematic interaction) transformed into the effect on resulting SDOF-response. This makes SA-amplification functions less sensitive as a function of period compared to transfer functions as a function of frequency. This is reflected in the results by a more gradual trend of the AF (refer to figure 3.11) compared to the trend of the TF (refer to figure 3.10) following from the same ground response models. This is illustrated by figure 3.11 that shows calculated SA-amplification function ratios.

Figure 3.10 1D site response analysis transfer function ratio (B-station profile/G-station profile)

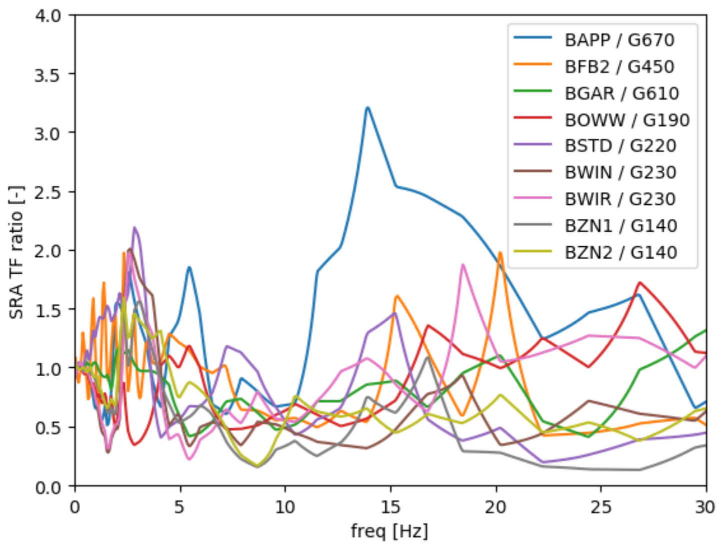

Figure 3.11 1D site response analysis amplification function ratio (B-station profile/G-station profile)

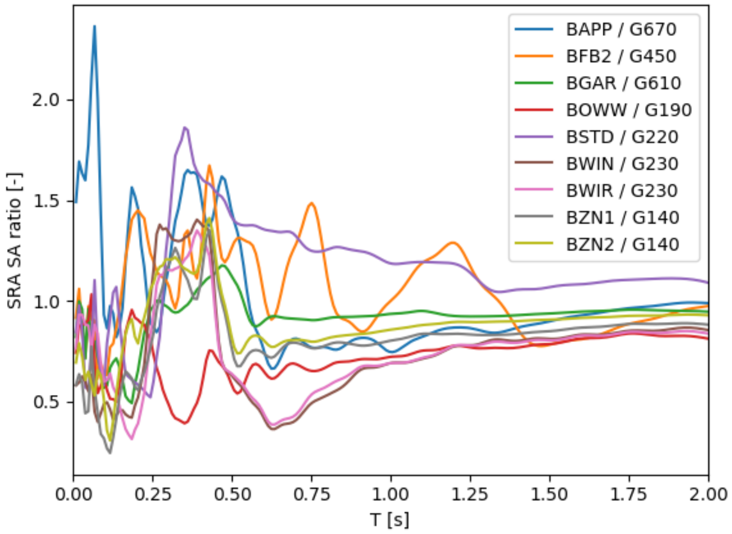


## 3.4.2 Summary table

Like in section 3.3, a summary table of the quality of corrected records is provided per station. The observations listed in the table are related to the specific consequences of the records correction in which site response analysis is taken into account, on top of the effects mentioned in section 3.3. For the high-level evaluation that is not specifically related to site response effects, one is referred to section 3.3.

Table 3.2 Summary of quality of records correction (with site response correction)

| B-station | G-station | Quality of FAS correction | Quality of SA-correction method Veletsos FAS TF | Quality of SA-correction method FEM 440 SA RRS |
|---|---|---|---|---|
| BAPP | G67 | SRA increases drift | for short periods ratio $TF_{SRA}$ seems too high, for long periods SRA improves results | for long periods SRA improves results |
| BFB2 | G45 | SRA results larger overshoot for f >20 Hz | SRA gives worse results | SRA gives worse results |
| BGAR | G61 | SRA contributes to drift correction | SRA impact seems to be too extreme | SRA impact seems to be too extreme |
| BOWW | G19 | SRA gives worse results | poor, impact by site response seems to be too extreme | poor, impact by site response seems to be too extreme |
| BSTD | G22 | high frequency deviations enlarged by SRA | including SRA improves the absolute SA-results | overshoot in period range 0.15 to 0.30 sec |
| BWIN | G23 | not clearly better or worse | mediocre, SA-peak better captured but shifted | mediocre, SA-peak better captured but shifted |
| BWIR | G23 | not clearly better or worse | mediocre, SA-peak better captured but shifted | mediocre, SA-peak better captured but shifted |
| BZN1 | G14 | SRA gives worse results | poor, ratio $TF_{SRA}$ for small periods well below 1.0, causing overshoot in corrected SA | poor, ratio $TF_{SRA}$ for small periods well below 1.0, causing overshoot in corrected SA |

| B-station | G-station | Quality of FAS correction | Quality of SA-correction method Veletsos FAS TF | Quality of SA-correction method FEM 440 SA RRS |
|---|---|---|---|---|
| BZN2 | G14 | SRA gives worse results | poor, TF, ratio $TF_{SRA}$ for small periods well below 1.0, causing overshoot in corrected SA | poor, ratio $TF_{SRA}$ for small periods well below 1.0, causing overshoot in corrected SA |

In general, it is concluded that including site response analysis in the comparison does not improve the consistency between B- and G-station records. Even for cases like BSTD-G220, that very clearly show a trend of fluctuating FAS-ratios (for all events), the site response correction factors based on the GMM v5 SRA model did not yield improved results. Further analysis towards possible explanations would be required to improve understanding.

### 3.4.3 Evaluations

**Cases BWIN-G230 and BWIR-G230**

BWIN and BWIR compared to G230 show a very similar typical trend. The G-station response spectra clearly show a much higher peak around period 0.1 - 0.2 sec. The site response transfer functions ratios from the STRATA-voxel stack realizations indicate TF and AF ratios well below 1.0 for the frequency range 5 to 10 Hz. This is fully contradictive to what was expected. By including the SRA-correction on B-station records, peak values of response spectra are better in line with the corresponding G-station records. However, a shift of this peak towards period 0.3 - 0.35 sec is observed. Possibly, the deep 1D-scenario for the voxel stack realisations includes misinterpretation of layering or stiffnesses of the soil resulting in an incorrect calculated ground response function.

Figure 3.12 SA-plots for cases BWIN-G230 and BWIR-G230 excluding (top) and including (bottom) SRA-correction

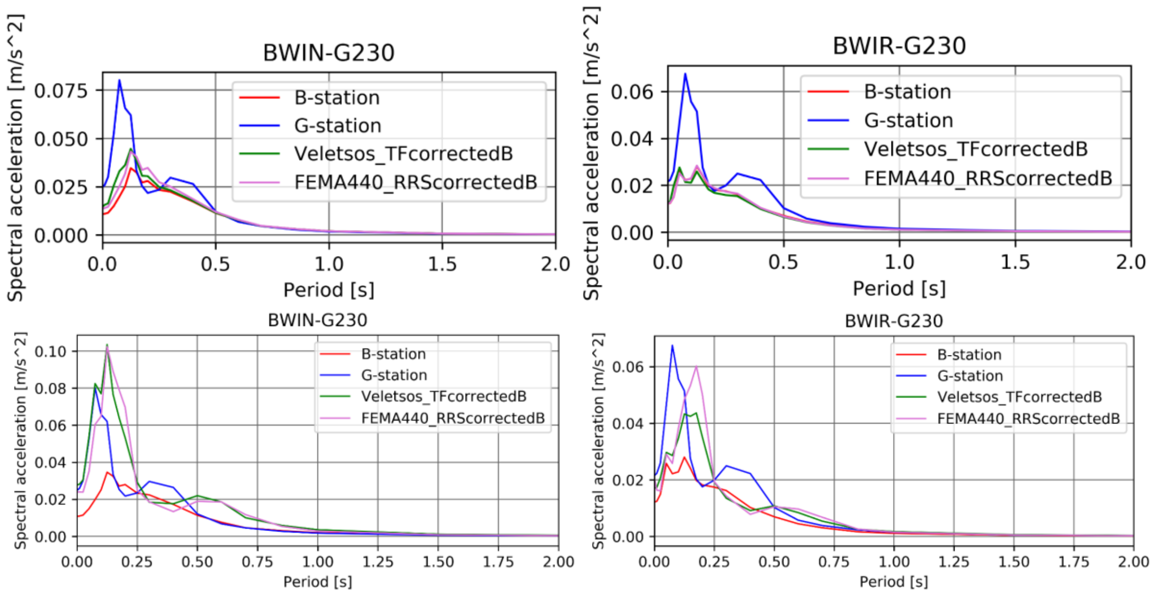


Cases BWIN-G230 and BWIR-G230 are the clearest examples of cases were a site response effect seems to be important (although a shift is observed). However, there may be other cases as well where the GMM v5 model-based SRA-corrections, seem not to contribute to the results, by simply being shifted in terms of frequency. Further detailed analysis of the actual site transfer functions based on Gxx0- and Gxx4-records evaluation, may provide improved corrections to account for site response.

# 4

# CONCLUSIONS AND RECOMMENDATIONS

## 4.1 Conclusions

This report describes an investigation to what extend available models in codes and literature for kinematic interaction effects are capable of explaining observed deviations between ground motions recorded by close B- and G-stations. 'Kinematic effects' is the term often used in international codes and literature to refer to deviations between free field ground response and foundation input motion response that result from non-synchronous base excitation, caused by different arrival times of the waves at different locations of a building foundation. Calculations have been performed based on two model formulations, being the transfer functions for translational motions due to kinematic interaction proposed by Veletsos (Veletsos, Prasad, & Wu, 1997) and the simplified ratio to response spectrum (RRS) expressions prescribed by FEMA 440 (NEHRP, 2005). The latter method has been adjusted to account for characteristic soils and ground motions observed in Groningen in order to obtain reasonable performance.

By modifying B-station recorded motions based on models and then comparing these equivalent corrected B-station motions to the coupled G-station motions, it has been evaluated if the models proposed by Veletsos and FEMA 440 do capture the observed deviations between B- and G-station recordings. Results are presented as Fourier Amplitude Spectrum (FAS)-ratios, spectral acceleration (SA)-ratios and absolute values of response spectra. Calculations and evaluation have been performed, excluding and including a correction related to ground response based on GMM v5 (Bommer , 2018) site amplification models.

It is concluded that the consistency of corrected B-station motions with G-station motions improves compared to uncorrected B-station motions, using both methods. Base slab averaging effects are frequency-dependent and tend to become more significant for higher frequencies, which could be explained by the increased effective size of a foundation relative to seismic wave lengths for high frequencies. This implies that stronger events will show more significant reductions of B-station motion compared to G-station motion. The relation to wavelength also indicates that the kinematic reduction of foundation motions increases with increasing size and mass of the foundation. This trend could be observed clearly from the recorded ground motions.

Including theoretical site amplification functions based on GMM v5 1D STRATA realisations in general does not further improve the results.

Based on the results of this study, it could be concluded that modification of B-station motions following the adjusted FEMA 440-procedure is expected to capture the difference between B-station recordings and the actual ground motion at the B-station location to some extent. The consistency between the results using either the adjusted FEMA 440-method and the Veletsos method confirm the validity of the adjustment proposed to the FEMA 440-formulation. For specific stations (or even specific events), deviation are observed, but the general framework seems applicable. By using this framework, the adjusted B-station motions are more consistent with G-station motions and are therefore an improved basis for GMM- or GMPE-development.

The inherent randomness in seismic ground motions in general implies that one actually should expect deviations when comparing stations. However, some trends are observed which indicate that there is an underlying mechanism which is not captured by the presently used simplified approach. These trends are discussed in the following section.

## 4.2 Recommendations

### 4.2.1 Possible model improvements

Although the results of the present study support the validity of the methods used for correction of B-station motions, there are a few specific aspects that are not yet captured well and possibly (when investigated further) could contribute to an improved model:

- A number of B- to G-station couples showed a trend being not consistent with simplified code-based mathematical models for kinematic interaction for frequencies above approximately 15 Hz. Models for kinematic interaction predict a monotonically decaying trend of translational foundation motions compared to 'clean' ground motions with increasing frequency. In contrast, a number of stations shows a clear increase in FAS-ratios for this high frequency range. Ground motion characteristics for Groningen seem to indicate that this frequency range of records is dominated by P-wave arrivals. This would imply that a different kinematic interaction model applies, given the corresponding wave lengths. This aspect needs further evaluation.
- Before starting the present study, the team expected to be able to explain the consistent fluctuations of FAS-ratios with frequency based on the difference between site amplification response of stations locations. This however could not be proven based on the records combined with GMM v5 site amplification models (adjusted based on latest SCPT-data for G-stations). This might indicate that the site amplification models deviate from the actual response, in terms of Fourier transfer functions. It is recommended to further investigate this by using actual recordings from G-station arrays (TF calculated from Gxx0- over Gxx4-motions).
- Another explanation for the fluctuations of FAS-ratios (and in general the recorded motion) may be related to building global rotation or torsion or local modes. This has not been investigated further at this stage because:
  - According to Veletsos (Veletsos, Prasad, & Wu, 1997) the amplitude of global torsion motions due to kinematic interaction effects is relatively low compared to potential translational reductions.
  - Evaluating rotation/torsion requires detailed data from the building superstructure, detailed consideration of incoming wave fields and a full soil-structure interaction analysis.

  This combined with the fact that B- and G-stations couples do typically have about 1 km interstation distance is not considered scientifically justified in relation to data available for validation.

### 4.2.2 Use of uncorrected or corrected motions

One very important remark should be made here: Depending on the use of a GMM or GMPE, the user needs either 'clean' ground motions or foundation input motions. A clear example of the former would be GMM-development in which the user of the GMM is accounting for kinematic interaction effects himself in the numerical simulations conducted for the specific case under consideration. A clear example of the latter is the use GMPE in combination with the Dutch guideline for vibration impact assessment SBR for damage assessment (SBR CURnet, 2017). SBR is based on comparison of foundation input motions. This implies that for such evaluations, one should either use a GMPE based on uncorrected B-station motions and corrected G-station motions and not account for kinematic effects separately, or use a GMPE based on corrected B-station recorded motions and uncorrected G-station motions and account for kinematic effects separately as part of the object based evaluation.

# 5

## REFERENCES


1 (2018. V5 Ground-Motion Model (GMM) for the Groningen Field, Re-issue with Assurance Letter. . (1977). Dynamic Behaviour of Embedded Foundations. Rpt. No. R77-33, Department of Civil Engineering., MIT, Cambridge, Massachusetts.

2 , J. (2003). Kinematic soil-structure interaction from strong motion recordings. Journal of Geotechnical & Geoenvironmental. Engineering, Vol. 129, No. 4, American Society of Civil Engineers, 323-335.

3 KNMI. (2013). The August 16, 2012 earthquake near Huizinge (Groningen), (2017). An integrated shear-wave velocity model for the Groningen gas field, The Netherlands, Bulletin Earthquake Engineering (2017) 15: 3555. https://doi.org/10.1007/s10518-017-0105-y.

4 NEHRP. (2005). FEMA 440, Improvement of Nonlinear Static Seismic Analysis Procedures.

5 NEHRP Consultants Joint Venture. (2012). NIST GCG 12-917-21, Soil Structure Interaction for Building Structures.

6 SBR CURnet. (2017). SBR Richtlijn A ‘Schade aan bouwwerken’.

7 Seister. (2019). Analysis of consistency between B- and G-stations records for induced events in the Groningen gas field, Draft Report, Document No. STR_FUG_18P17_01.

8 Veletsos, A., & Prasad, A. (1989). Seismic interaction of structures and soils: stochastic approach. Journal of Structural Engineering, Vol. 115, No.4, American Society of Civil Engineers, 935-956.

9 Veletsos, A., Prasad, A., & Wu, W. (1997). Transfer functions for rigid rectangular foundations. Journal of Earthquake Engineering & Structural Dynamics, Vol 26, No. 1, 5-17.

10 Witteveen+Bos. (2019a). Investigation of malfunctioning earthquake recording stations for Groningen Earthquake events of the period 2014-2018, Staatstoezicht op de Mijnen, ref. 113982/19-008.330, final version.

11 Witteveen+Bos. (2019b). Dynamic amplification effects for B-stations due to building response.

12 Staatstoezicht op de mijnen, ref. 113982/19-009.783.

# Appendices

# APPENDIX: CALCULATION RESULTS - REFERENCE RESULTS

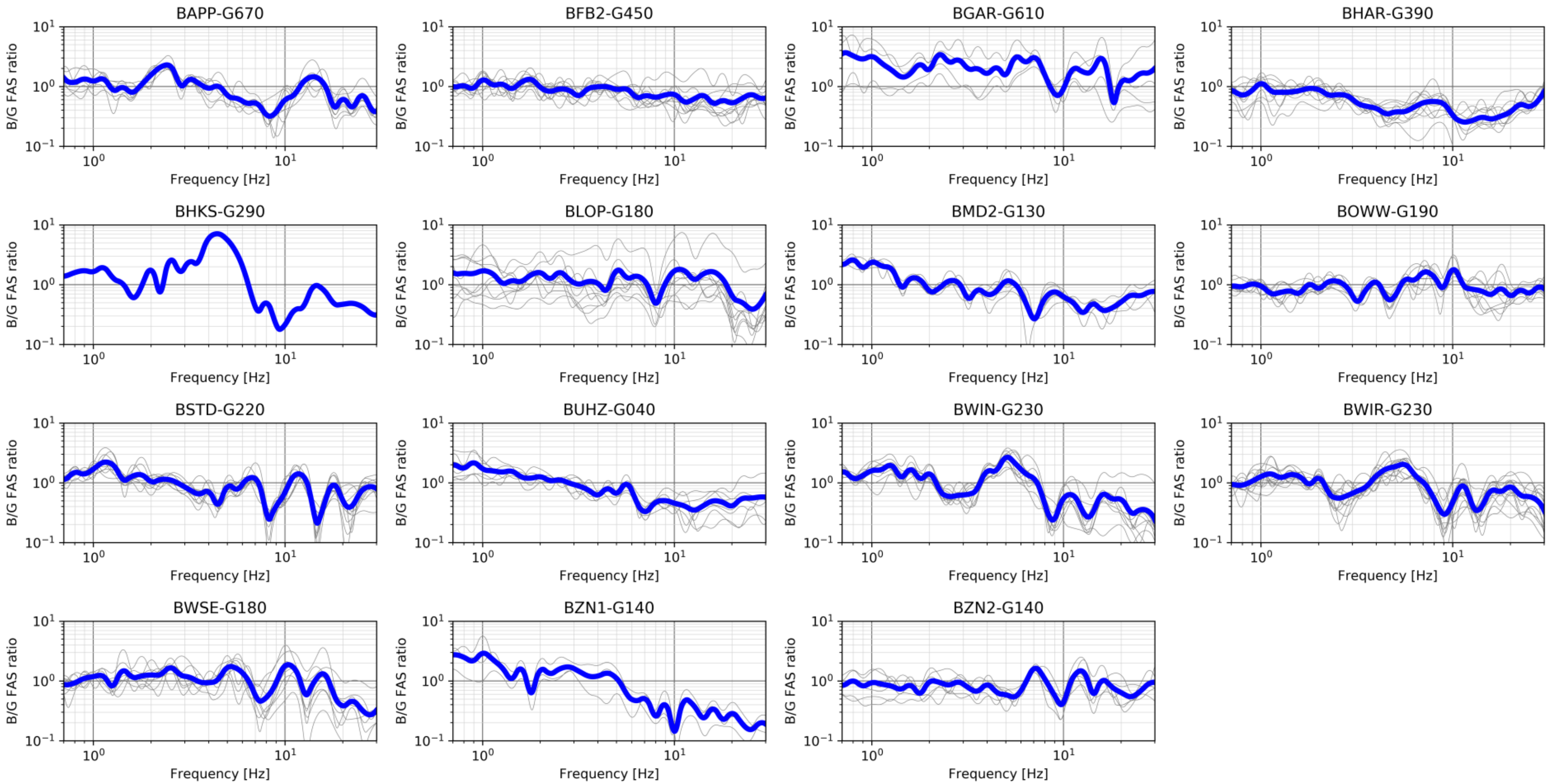
BAPP-G670
BFB2-G450
BGAR-G610
BHAR-G390
BHKS-G290
BLOP-G180
BMD2-G130
BOWW-G190
BSTD-G220
BUHZ-G040
BWIN-G230
BWIR-G230
BWSE-G180
BZN1-G140
BZN2-G140
B/G FAS ratio
Frequency [Hz]
$10^{1}$
$10^{0}$
$10^{-1}$

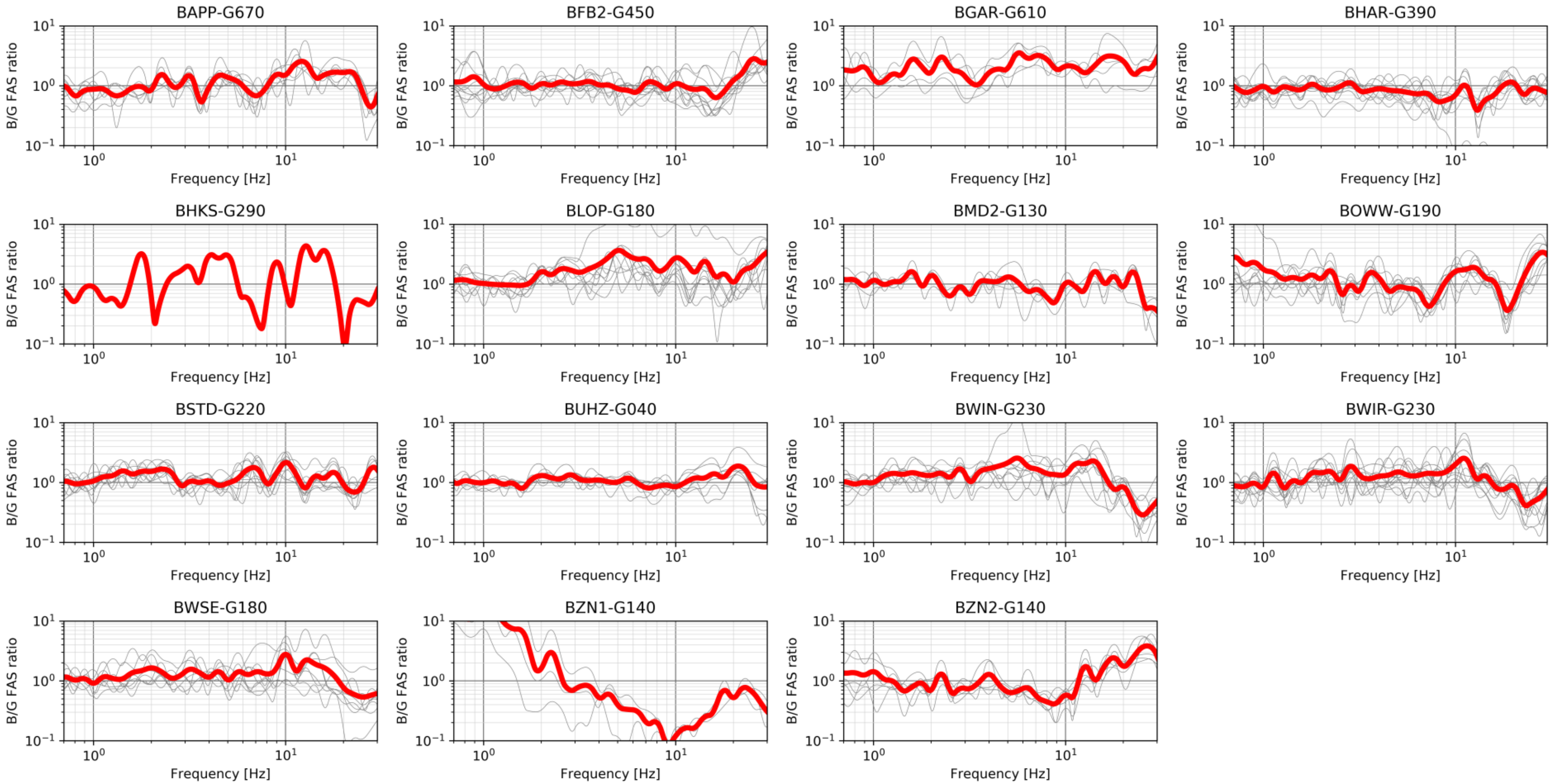
BAPP-G670
BFB2-G450
BGAR-G610
BHAR-G390
BHKS-G290
BLOP-G180
BMD2-G130
BOWW-G190
BSTD-G220
BUHZ-G040
BWIN-G230
BWIR-G230
BWSE-G180
BZN1-G140
BZN2-G140
B/G FAS ratio
Frequency [Hz]

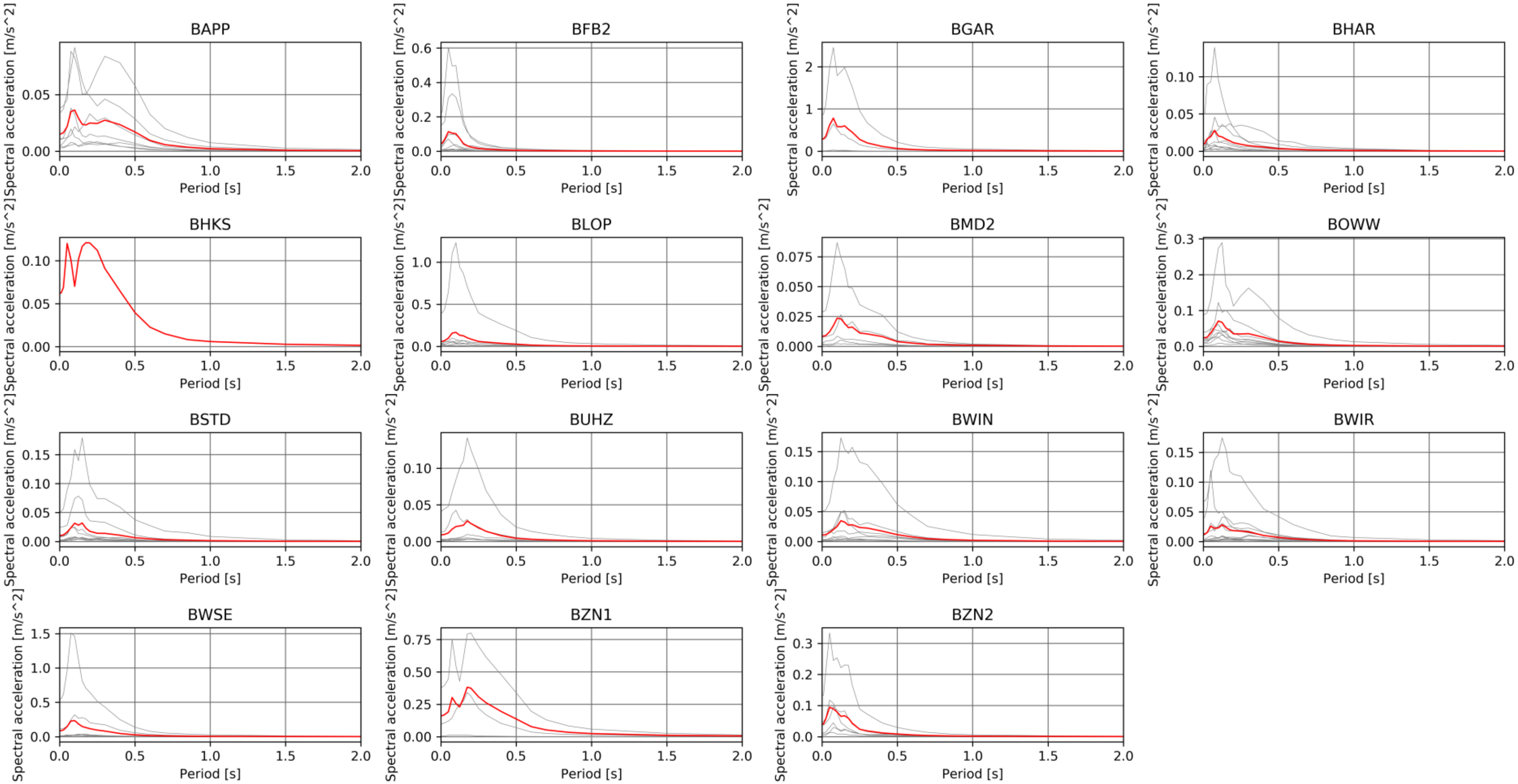
BAPP
BFB2
BGAR
BHAR
BHKS
BLOP
BMD2
BOWW
BSTD
BUHZ
BWIN
BWIR
BWSE
BZN1
BZN2
Spectral acceleration [m/s^2]
Period [s]

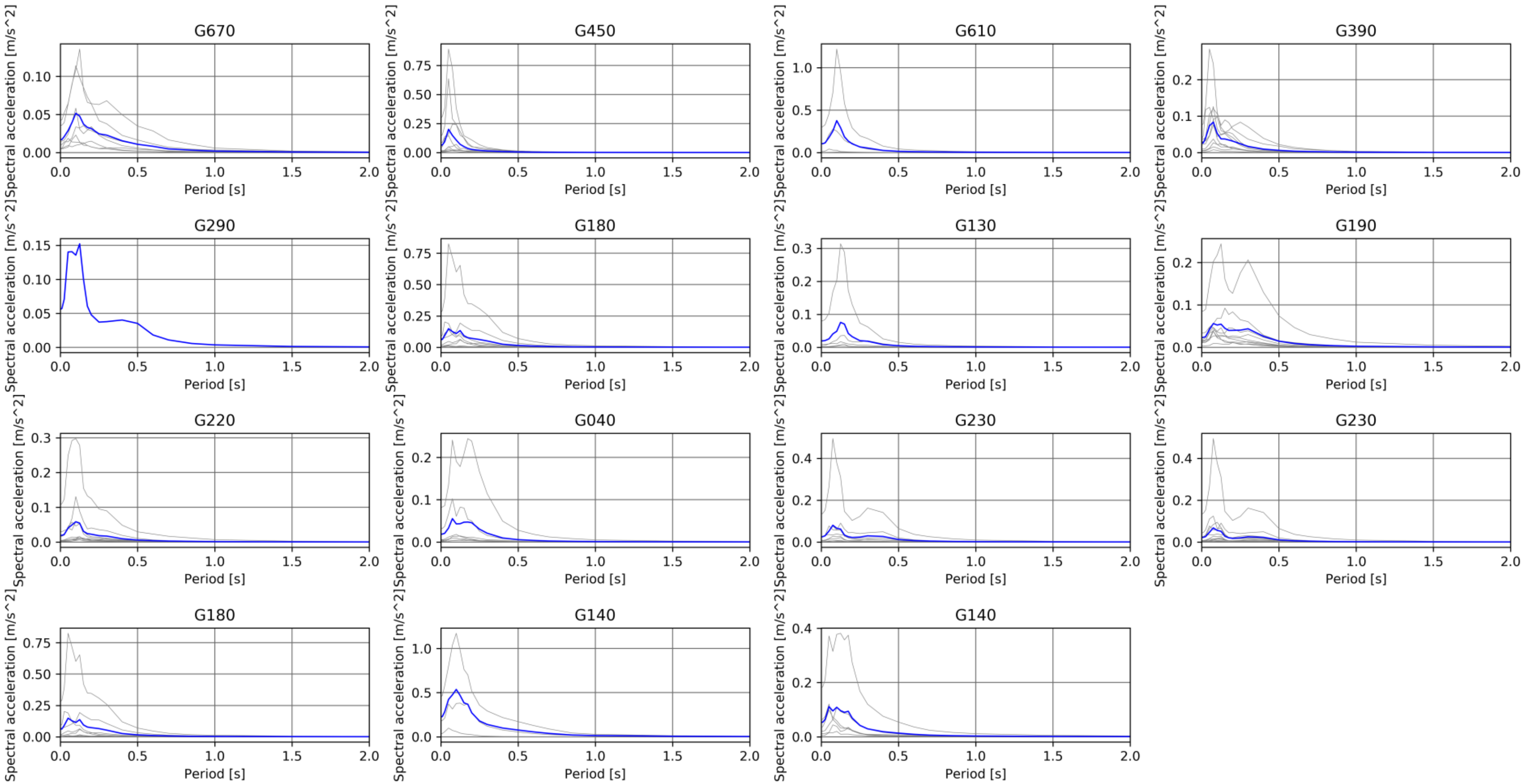
G670
G450
G610
G390
G290
G180
G130
G190
G220
G040
G230
G230
G180
G140
G140
Spectral acceleration [m/s^2]
Period [s]

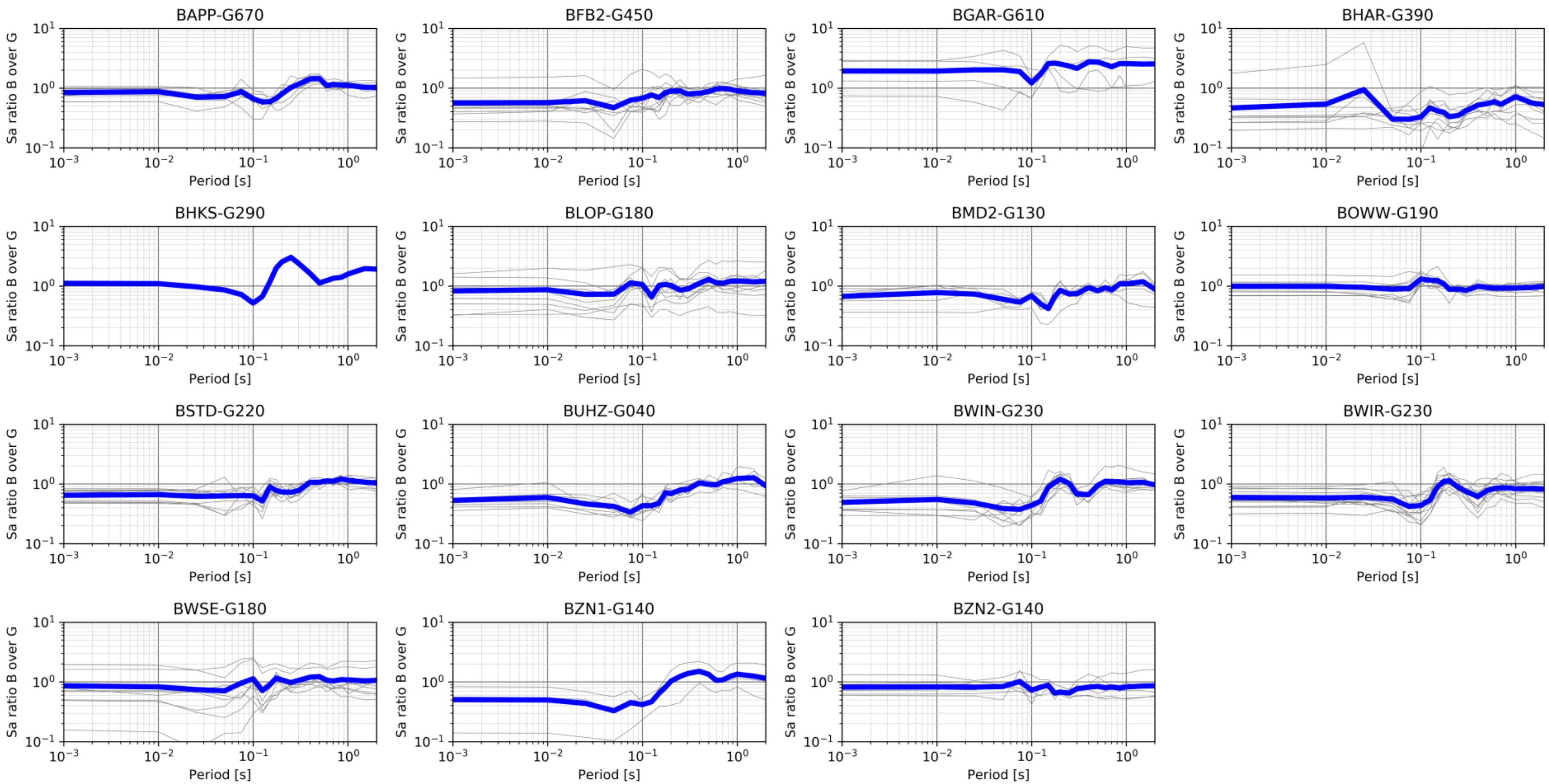

BAPP-G670
BFB2-G450
BGAR-G610
BHAR-G390
BHKS-G290
BLOP-G180
BMD2-G130
BOWW-G190
BSTD-G220
BUHZ-G040
BWIN-G230
BWIR-G230
BWSE-G180
BZN1-G140
BZN2-G140
Sa ratio B over G
Period [s]
$10^{-3}$
$10^{-2}$
$10^{-1}$
$10^{0}$
$10^{1}$

# II

## APPENDIX: CALCULATION RESULTS - B-STATION RECORDS MODIFIED, EXCLUDING GROUND RESPONSE CORRECTION

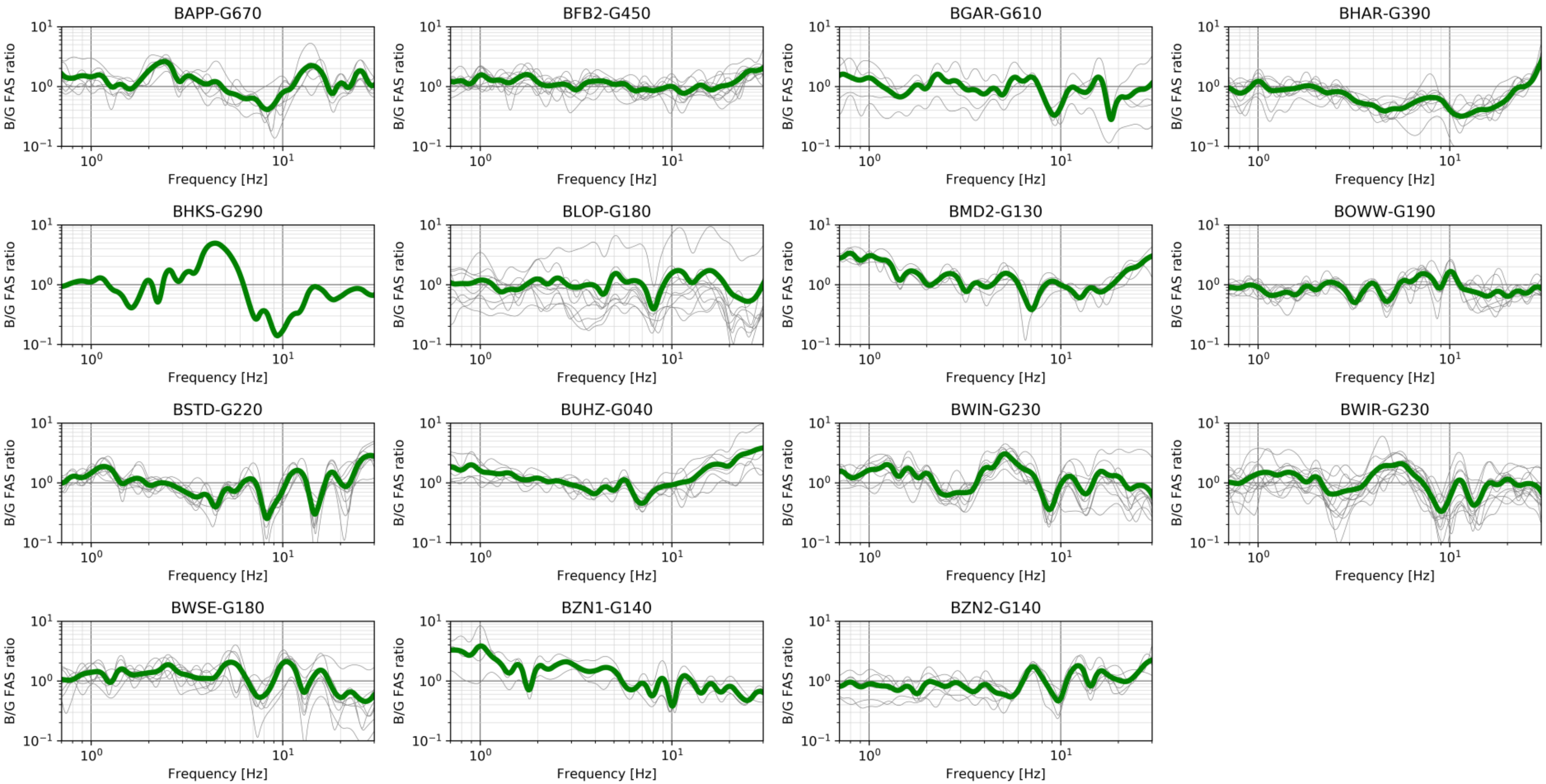

BAPP-G670
BFB2-G450
BGAR-G610
BHAR-G390
BHKS-G290
BLOP-G180
BMD2-G130
BOWW-G190
BSTD-G220
BUHZ-G040
BWIN-G230
BWIR-G230
BWSE-G180
BZN1-G140
BZN2-G140
B/G FAS ratio
Frequency [Hz]
$10^{-1}$
$10^{0}$
$10^{1}$

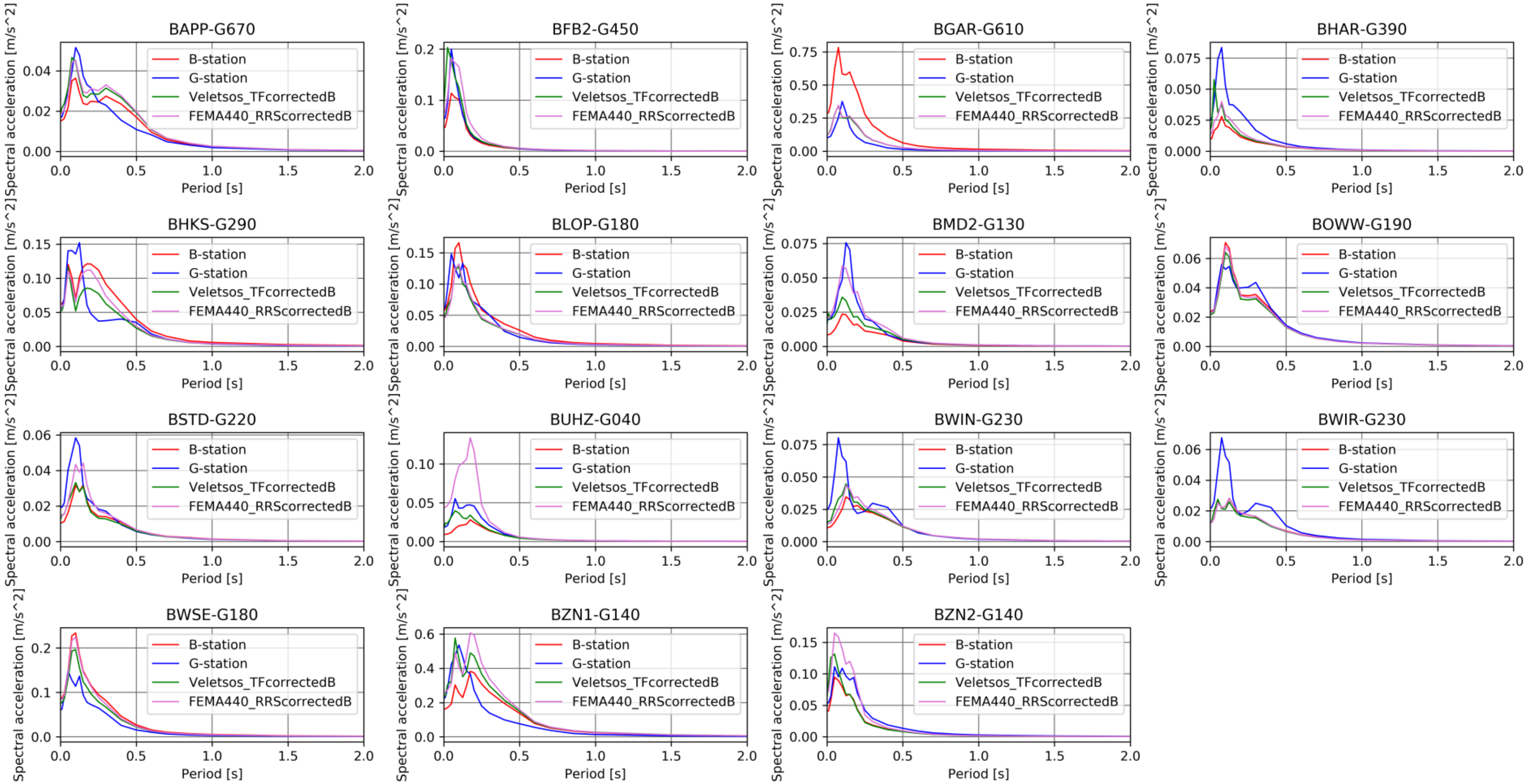
BAPP-G670
BFB2-G450
BGAR-G610
BHAR-G390
BHKS-G290
BLOP-G180
BMD2-G130
BOWW-G190
BSTD-G220
BUHZ-G040
BWIN-G230
BWIR-G230
BWSE-G180
BZN1-G140
BZN2-G140
B-station
G-station
Veletsos_TFcorrectedB
FEMA440_RRScorrectedB
Spectral acceleration [m/s^2]
Period [s]

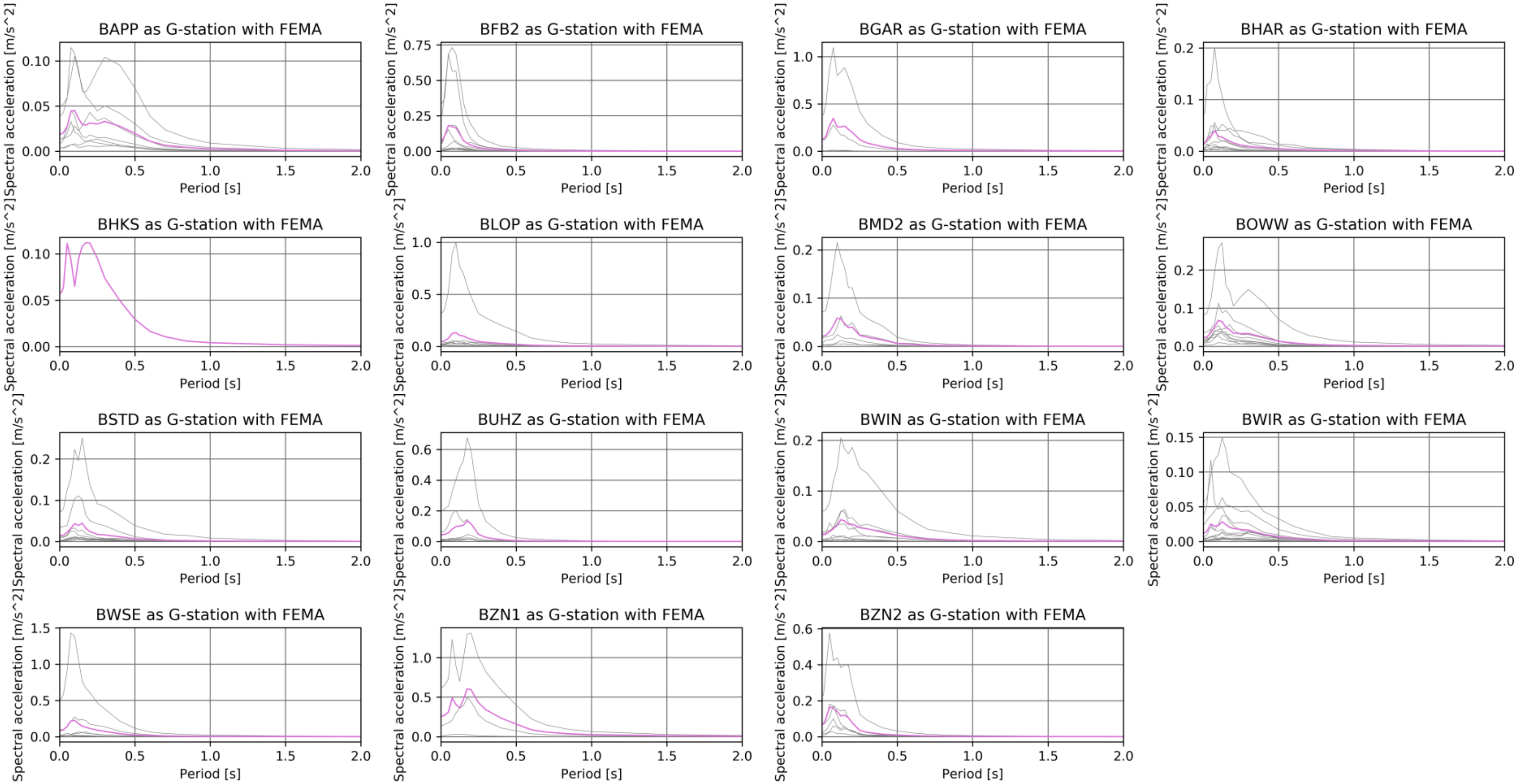
BAPP as G-station with FEMA
BFB2 as G-station with FEMA
BGAR as G-station with FEMA
BHAR as G-station with FEMA
BHKS as G-station with FEMA
BLOP as G-station with FEMA
BMD2 as G-station with FEMA
BOWW as G-station with FEMA
BSTD as G-station with FEMA
BUHZ as G-station with FEMA
BWIN as G-station with FEMA
BWIR as G-station with FEMA
BWSE as G-station with FEMA
BZN1 as G-station with FEMA
BZN2 as G-station with FEMA
Spectral acceleration [m/s^2]
Period [s]

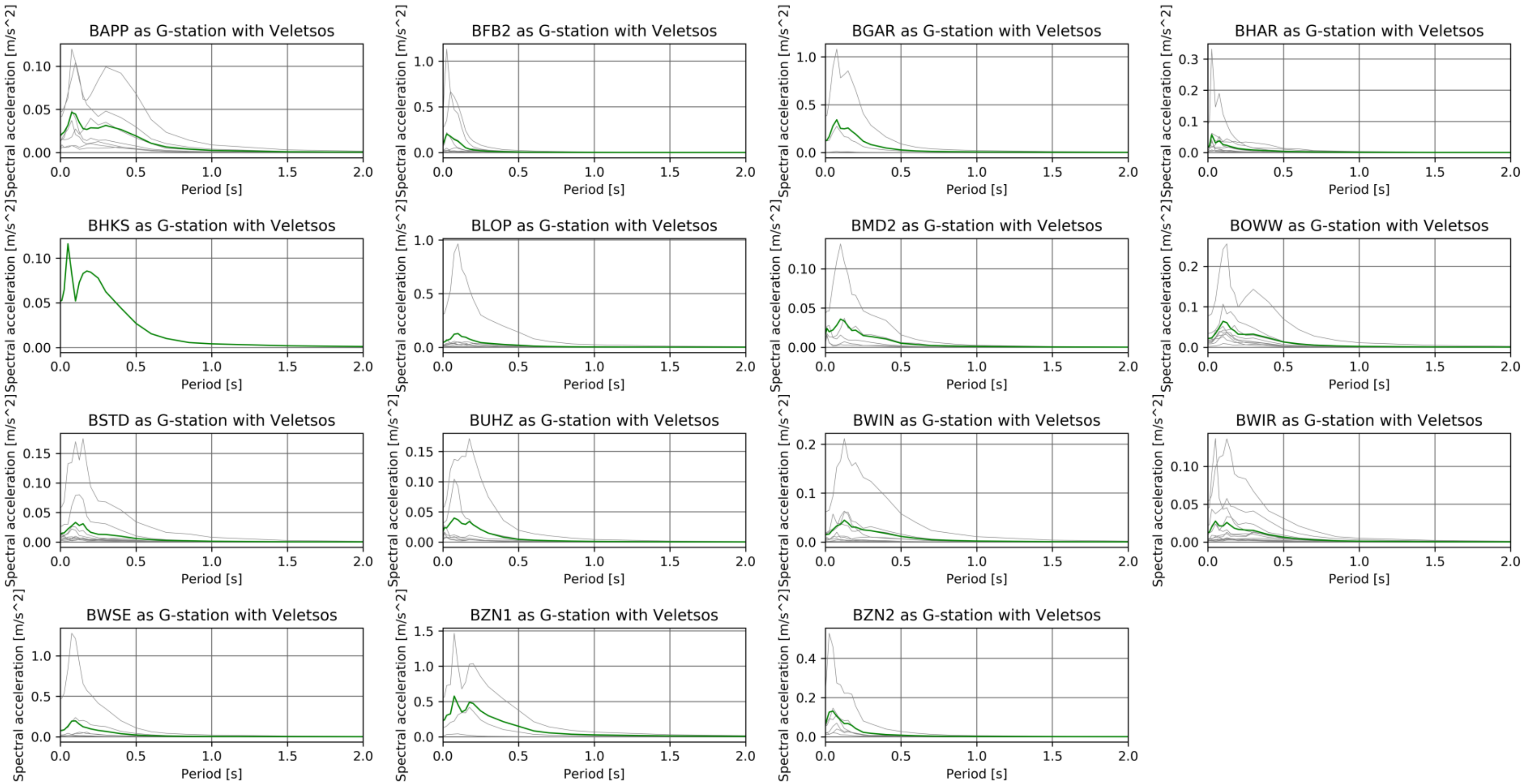
BAPP as G-station with Veletsos
BFB2 as G-station with Veletsos
BGAR as G-station with Veletsos
BHAR as G-station with Veletsos
BHKS as G-station with Veletsos
BLOP as G-station with Veletsos
BMD2 as G-station with Veletsos
BOWW as G-station with Veletsos
BSTD as G-station with Veletsos
BUHZ as G-station with Veletsos
BWIN as G-station with Veletsos
BWIR as G-station with Veletsos
BWSE as G-station with Veletsos
BZN1 as G-station with Veletsos
BZN2 as G-station with Veletsos
Spectral acceleration [m/s^2]
Period [s]

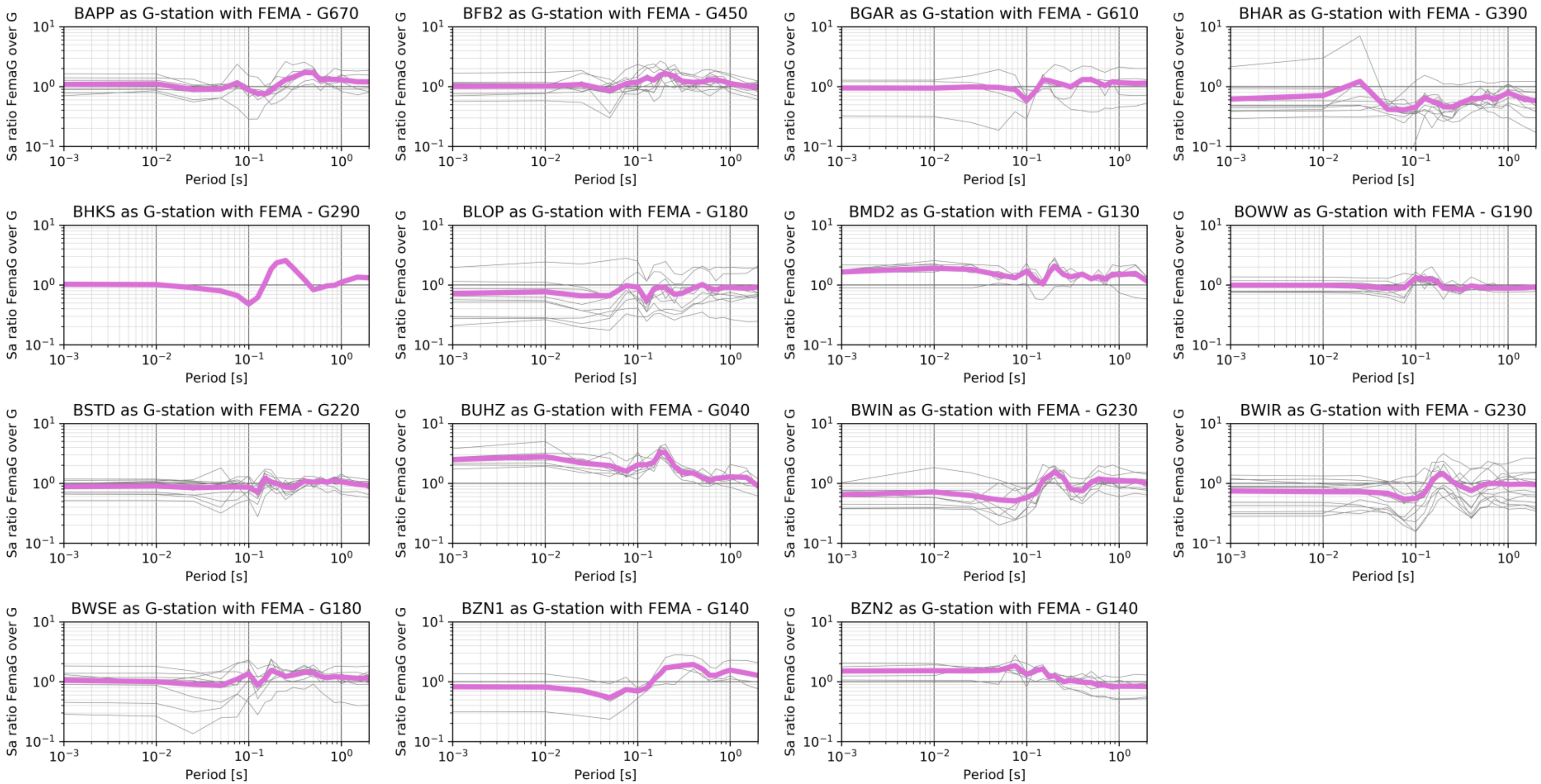
BAPP as G-station with FEMA - G670
BFB2 as G-station with FEMA - G450
BGAR as G-station with FEMA - G610
BHAR as G-station with FEMA - G390
BHKS as G-station with FEMA - G290
BLOP as G-station with FEMA - G180
BMD2 as G-station with FEMA - G130
BOWW as G-station with FEMA - G190
BSTD as G-station with FEMA - G220
BUHZ as G-station with FEMA - G040
BWIN as G-station with FEMA - G230
BWIR as G-station with FEMA - G230
BWSE as G-station with FEMA - G180
BZN1 as G-station with FEMA - G140
BZN2 as G-station with FEMA - G140
Sa ratio FemaG over G
Period [s]
$10^{-1}$
$10^{0}$
$10^{1}$
$10^{-3}$
$10^{-2}$
$10^{-1}$
$10^{0}$

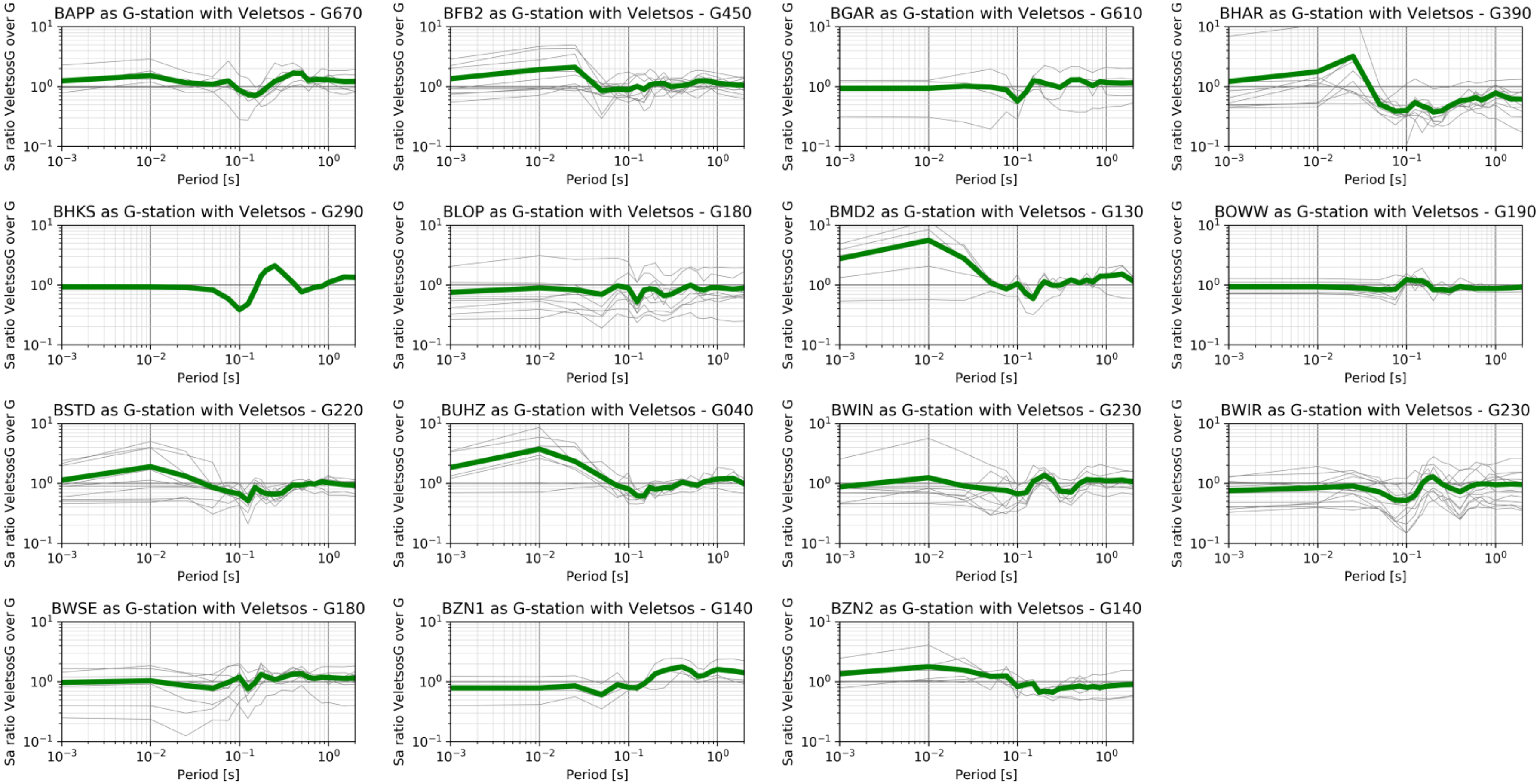

BAPP as G-station with Veletsos - G670
BFB2 as G-station with Veletsos - G450
BGAR as G-station with Veletsos - G610
BHAR as G-station with Veletsos - G390
BHKS as G-station with Veletsos - G290
BLOP as G-station with Veletsos - G180
BMD2 as G-station with Veletsos - G130
BOWW as G-station with Veletsos - G190
BSTD as G-station with Veletsos - G220
BUHZ as G-station with Veletsos - G040
BWIN as G-station with Veletsos - G230
BWIR as G-station with Veletsos - G230
BWSE as G-station with Veletsos - G180
BZN1 as G-station with Veletsos - G140
BZN2 as G-station with Veletsos - G140
Sa ratio VeletsosG over G
Period [s]

III

# APPENDIX: CALCULATION RESULTS - B-STATION RECORDS MODIFIED, INCLUDING GROUND RESPONSE CORRECTION

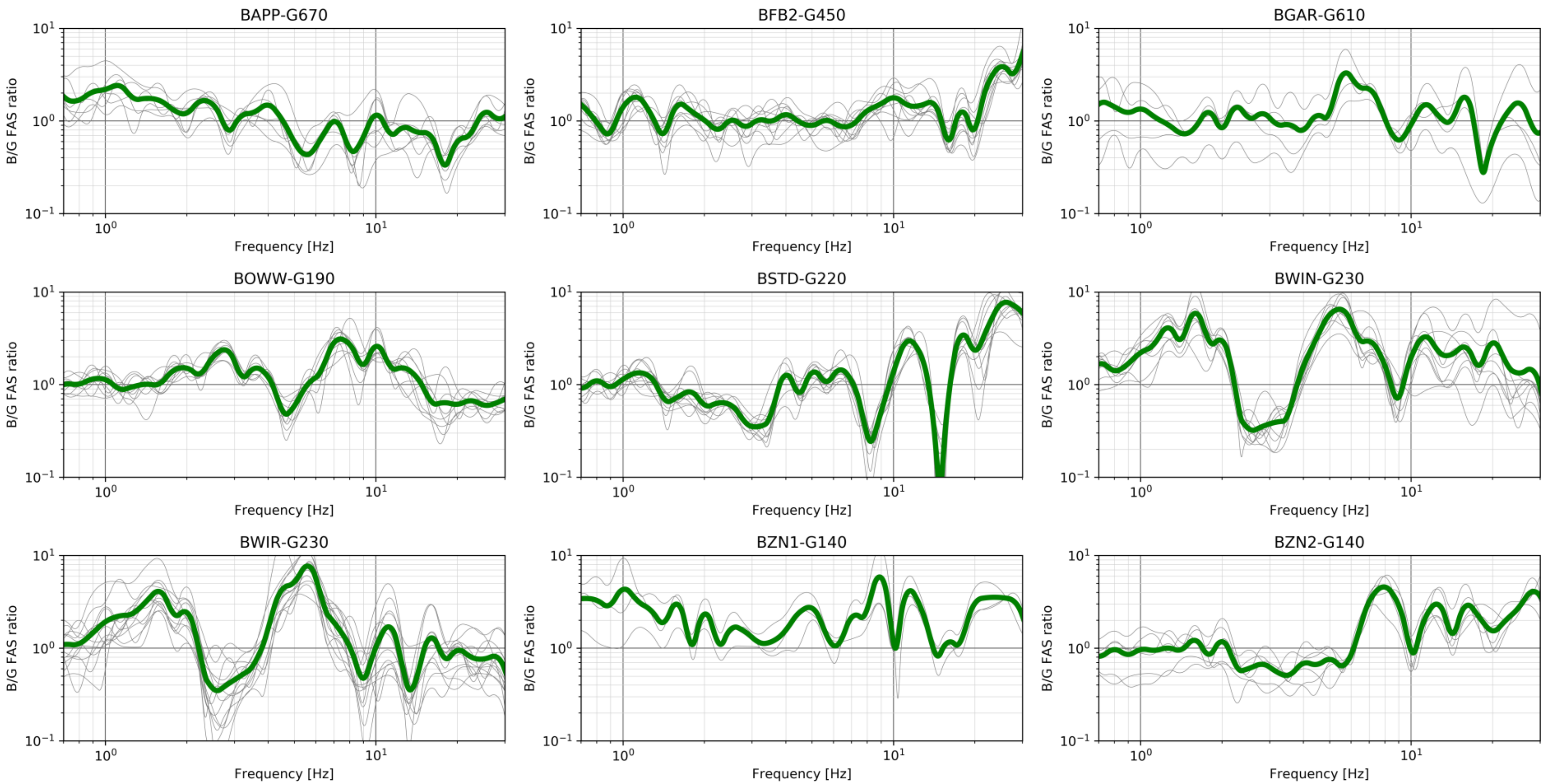
BAPP-G670
BFB2-G450
BGAR-G610
BOWW-G190
BSTD-G220
BWIN-G230
BWIR-G230
BZN1-G140
BZN2-G140
B/G FAS ratio
Frequency [Hz]
$10^{1}$
$10^{0}$
$10^{-1}$

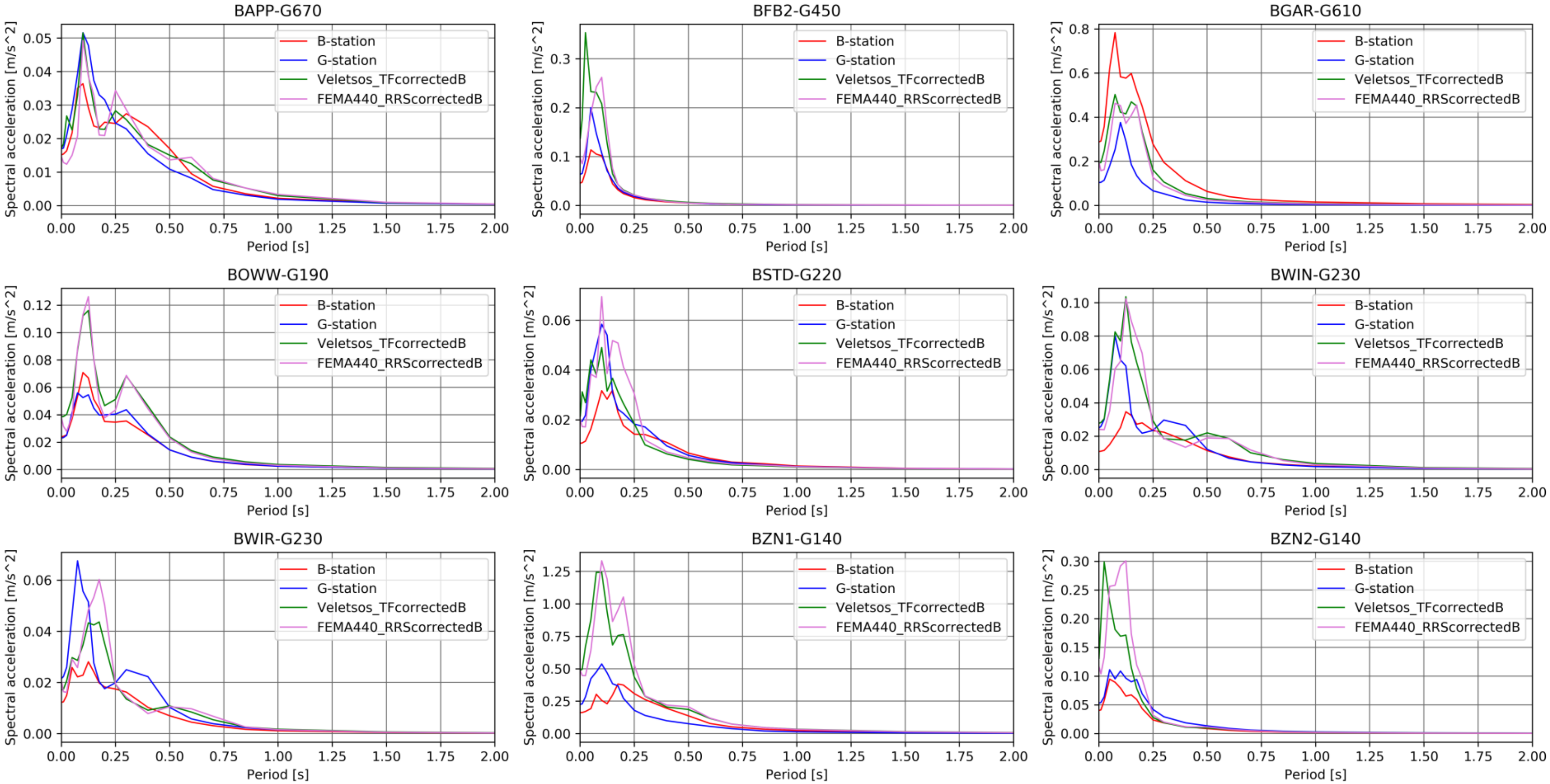
BAPP-G670
BFB2-G450
BGAR-G610
BOWW-G190
BSTD-G220
BWIN-G230
BWIR-G230
BZN1-G140
BZN2-G140
B-station
G-station
Veletsos_TFcorrectedB
FEMA440_RRScorrectedB
Spectral acceleration [m/s^2]
Period [s]

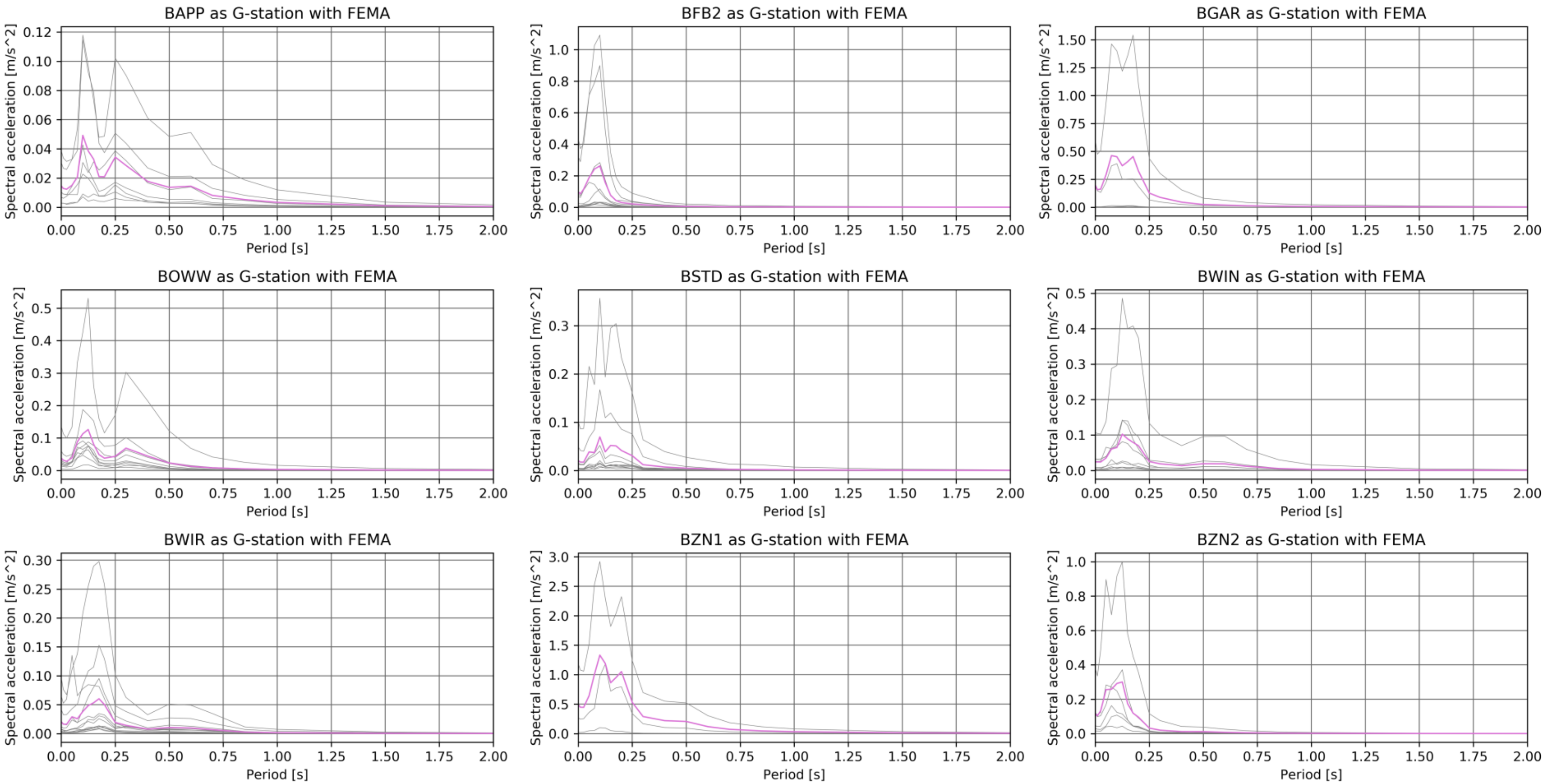

BAPP as G-station with FEMA
BFB2 as G-station with FEMA
BGAR as G-station with FEMA
BOWW as G-station with FEMA
BSTD as G-station with FEMA
BWIN as G-station with FEMA
BWIR as G-station with FEMA
BZN1 as G-station with FEMA
BZN2 as G-station with FEMA
Spectral acceleration [m/s^2]
Period [s]

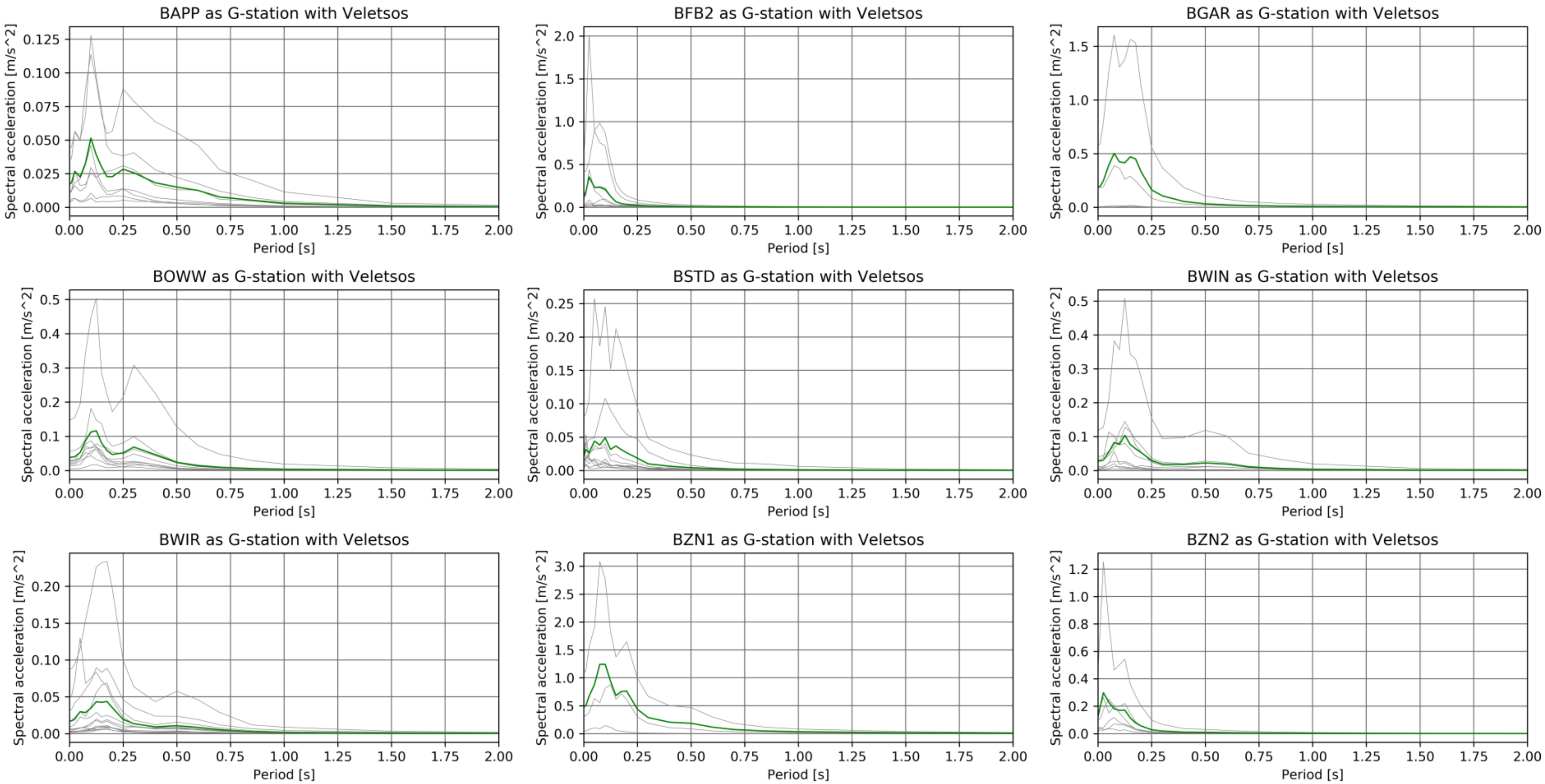
BAPP as G-station with Veletsos
BFB2 as G-station with Veletsos
BGAR as G-station with Veletsos
BOWW as G-station with Veletsos
BSTD as G-station with Veletsos
BWIN as G-station with Veletsos
BWIR as G-station with Veletsos
BZN1 as G-station with Veletsos
BZN2 as G-station with Veletsos
Spectral acceleration [m/s^2]
Period [s]
0.00
0.25
0.50
0.75
1.00
1.25
1.50
1.75
2.00

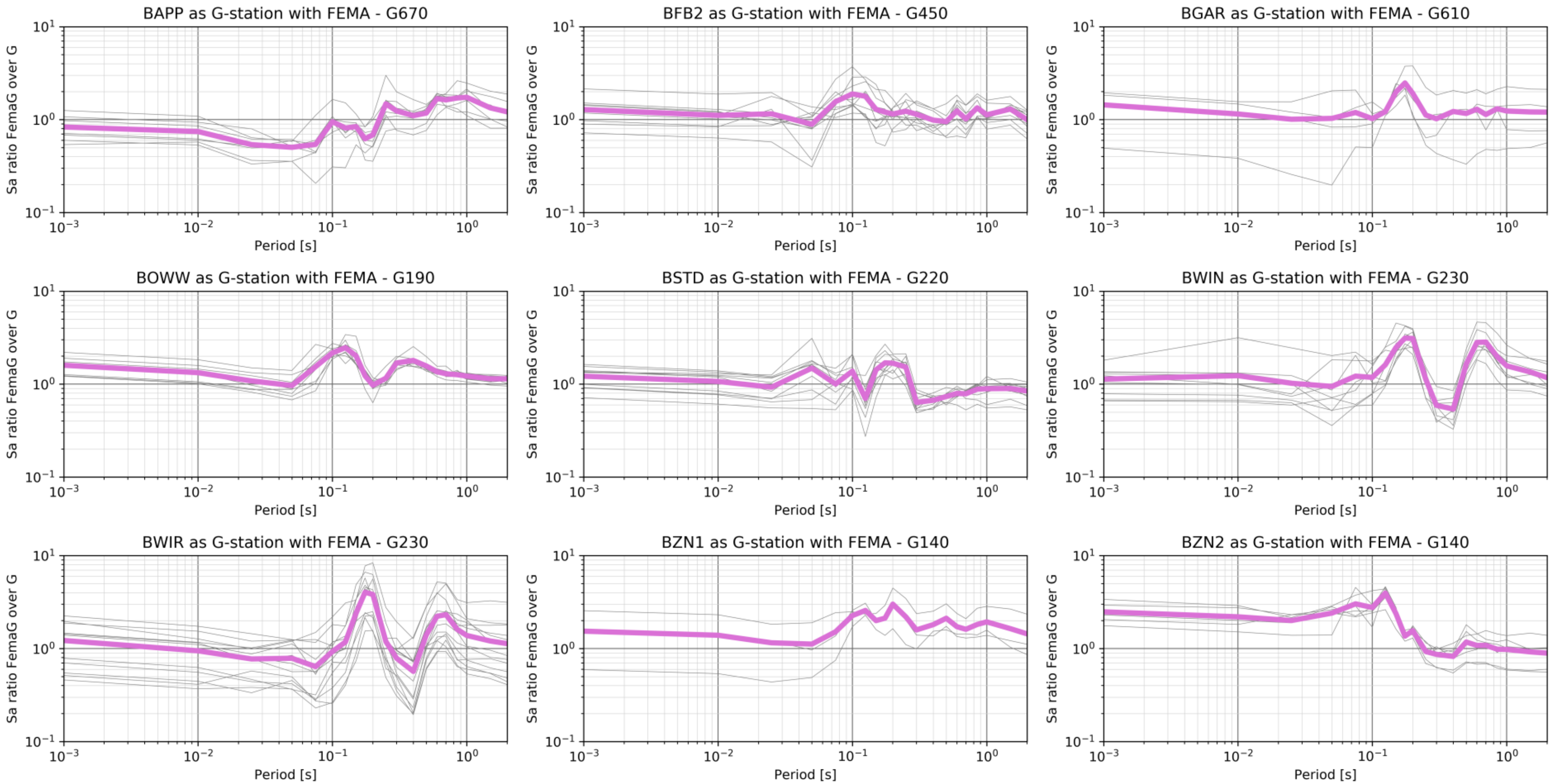

BAPP as G-station with FEMA - G670
BFB2 as G-station with FEMA - G450
BGAR as G-station with FEMA - G610
BOWW as G-station with FEMA - G190
BSTD as G-station with FEMA - G220
BWIN as G-station with FEMA - G230
BWIR as G-station with FEMA - G230
BZN1 as G-station with FEMA - G140
BZN2 as G-station with FEMA - G140
Sa ratio FemaG over G
Period [s]
$10^{-1}$
$10^{0}$
$10^{1}$
$10^{-3}$
$10^{-2}$

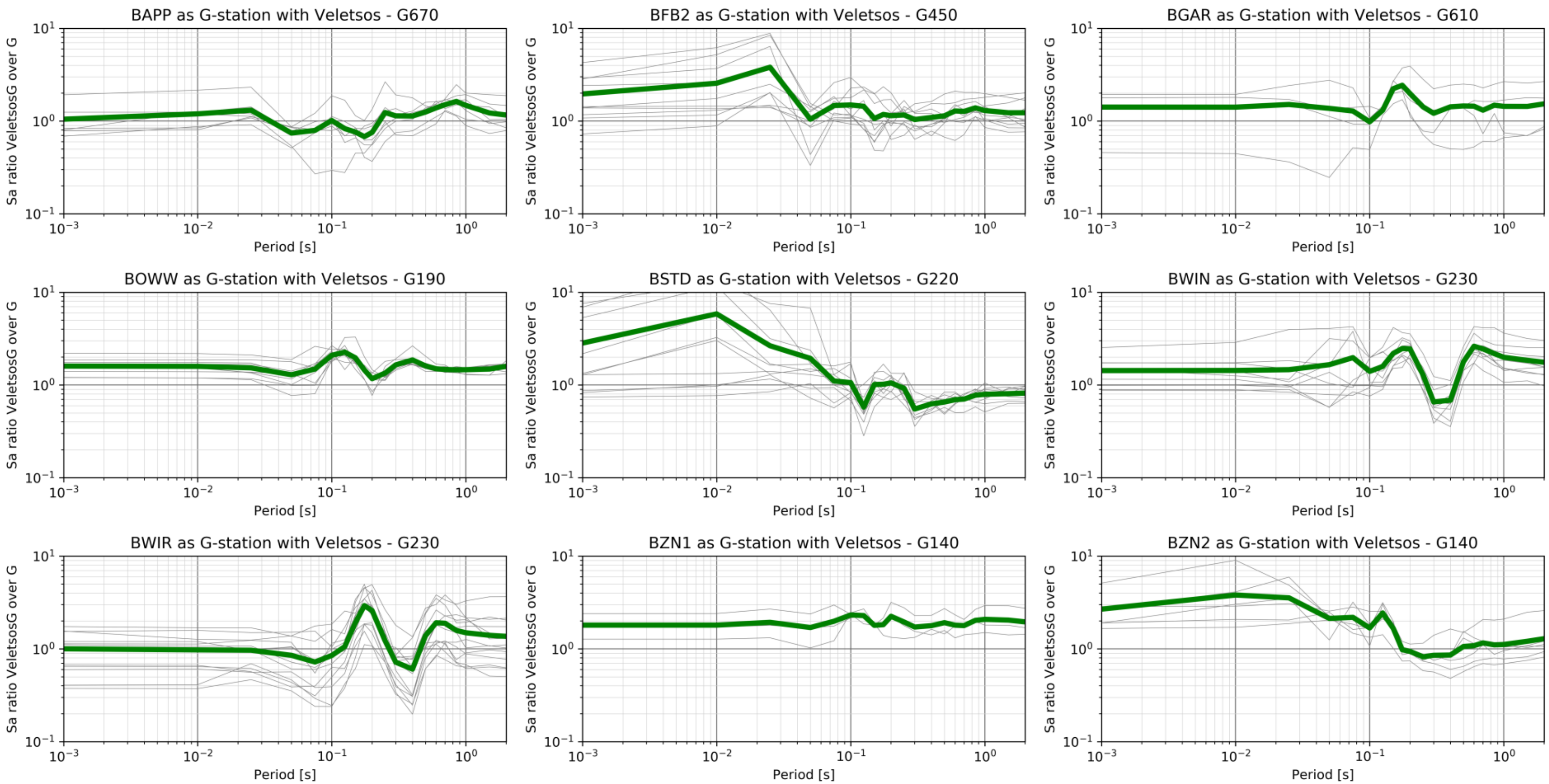
BAPP as G-station with Veletsos - G670
BFB2 as G-station with Veletsos - G450
BGAR as G-station with Veletsos - G610
BOWW as G-station with Veletsos - G190
BSTD as G-station with Veletsos - G220
BWIN as G-station with Veletsos - G230
BWIR as G-station with Veletsos - G230
BZN1 as G-station with Veletsos - G140
BZN2 as G-station with Veletsos - G140
Sa ratio VeletsosG over G
Period [s]